Aalto University
School of Chemical
Technology

School of Chemical Technology
Degree Programme of Forest Products Technology

Niko Heikkinen

NON-SPECIFIC METHOD FOR TIME-RESOLVED FLUORESCENCE ION DETECTION

Master's thesis for the degree of Master of Science in Technology submitted for inspection, Espoo, 23 November, 2015.

Supervisor **Professor Jouni Paltakari**

Instructor **M.Sc. Joonas Siivonen**

Aalto-yliopisto
Kemian tekniikan korkeakoulu

Aalto-yliopisto, PL 11000, 00076 AALTO
www.aalto.fi
Diplomityön tiivistelmä

Tekijä Niko Heikkinen

Työn nimi Non-specific method for time-resolved fluorescence ion detection

Laitos Puunjalostustekniikan laitos

Professuuri Paperi- ja painatustekniikka **Professuurikoodi** Puu-21

Työn valvoja Jouni Paltakari

Työn ohjaaja(t)/Työn tarkastaja(t) Joonas Siivonen / Sakari Kulmala

Päivämäärä 9.11.2015 **Sivumäärä** 53+7 **Kieli** Englanti

Tiivistelmä

Vesi liittyy olennaisesti lukuisiin teollisuuden prosesseihin, joista öljyteollisuus ei veden osalta poikkea. Öljyteollisuudessa esiintyy vettä erilaisissa prosesseissa yhtä paljon kuin hiilivetyjäkin. Koska näitä nesteitä kuljetetaan putkistojen välityksellä, johtaa veden suuri määrä ajoittain ongelmiin. Erityisen ongelmallisia ovat veteen liuenneet ionit, jotka aiheuttavat sakkaantuessaan merkittäviä taloudellisia menetyksiä rajoittamalla virtaamaa tuotantoputkistoissa.

Tämän työn tarkoitus oli kehittää menetelmä yleisimpien sakkaavien ionien konsentraatioiden määrittämiseksi öljyteollisuuden tuotantovesinäytteistä. Sakkaavien ionien määrityksen avulla oli mahdollista arvioida tuotantovesien sakkauspotentiaalia, jonka tunteminen on hyödyllistä tietoa öljyntuotantoprosessin ylläpitäjälle.

Tässä diplomityössä tutkittiin aikaerotteiseen fluoresenssiin (TRF) perustuvan analyysimenetelmän mahdollisuuksia määrittää sakkaavien ionien konsentraatioita synteettisistä ja oikeista tuotantovesinäytteistä. Fluoresenssimenetelmän kehittämiseen kuului soveltuvien pintakemioiden arvioiminen ja valinta varsinaista fluoresenssimittausta varten sekä tilastollisen ennustemallin kehittäminen eri ionikonsentraatioiden arvioimiseksi.

Tämän diplomityön tulokset osoittavat ionikonsentraatioiden mittaamisen näytematriiseista mahdolliseksi aikarajoitteiseen fluoresenssimittaukseen perustuvan teknologian avulla. Kehitettyjen menetelmien avulla on mahdollista luoda mittausjärjestelmä nestenäytteiden sakkaamispotentiaalin tunnistamiseksi.

Avainsanat Aikaerotteinen fluoresenssi, tuotantovesi, liuos-sormenjälki

Aalto University
School of Chemical
Technology

Aalto University, P.O. BOX 11000, 00076
AALTO
www.aalto.fi

Abstract of master's thesis

Author Niko Heikkinen

Title of thesis Non-specific method for time-resolved fluorescence ion detection

Department Forest Products Technology

Professorship Paper and Printing Technology **Code of professorship** Puu-21

Thesis supervisor Jouni Paltakari

Thesis advisor(s) / Thesis examiner(s) Joonas Siivonen / Sakari Kulmala

Date 9.11.2015 **Number of pages** 53+7 **Language** English

Abstract

Water in one form or another is present within countless manufacturing processes. In an oil extraction process, the volume of water is typically equal to the produced hydrocarbons and can even exceed the amount of extracted oil significantly. The large volumes of water, known as produced water, inflict problems. These problems are mainly related to dissolved ions that produced water is carrying. In oil production and several other industries, where pipelines are used to transport water, in suitable conditions, ions within the water will precipitate and form scale. Within a pipeline, scale may accumulate and disturb the liquid flow through the pipeline.

In order to assess the scale potential, this thesis develops a fluorescence based analytical method for identifying components that can induce scale within produced water. In this thesis, the studied water samples are called produced water, which is an oil extraction by-product. This thesis examines the technique of time-resolved photoluminescence to develop a non-specific assay method for identifying several ions that may cause scale accumulation in production pipelines. The developed method was used to analyse both synthetic and field produced water samples.

The results of this thesis indicate that thorough study of suitable assay components enables the possibility to create a measurement protocol to evaluate ion concentrations in a produced water sample. The quantification of ion concentrations allows the evaluation of scale potential in a production pipeline. This evaluation can be used to assess the need for treating chemical to prevent scale accumulation within the pipelines.

Keywords time-resolved fluorescence, produced water, liquid fingerprint

Preface

This study was performed at the Chemistry R&D Department of Aqsens Oy in Turku during the period of May-October 2015.

I would like to thank my supervisor Jouni Paltakari who gave me motivation and advice, as well as directed my mind-set towards analytical thinking and spurred my thirst for knowledge. The most important contributor to my work was Joonas Siivonen, who helped me resiliently during this thesis and inspired me to continuously learn new things.

Because of this thesis, I moved into a new city, however the settling to a new environment was extremely easy with the help of my colleagues, such as Mirva Lehmusto, Marianne Lähderanta, Joonas Wahrman, Satu Tiittanen, Piia Mäkinen, Paul Mundill and Pave Väisänen. I am grateful for your valuable guidance and assistance. Furthermore, I would like to express my gratitude to the persons made this thesis possible through funding and investing on Aqsens Oy.

Finally, I am thankful for the support and joy from my family and friends who provide me a well-balanced state of mind for the good and bad days of my life. In addition, I would like to thank my bicycle, which carried me every day, regardless of the cold summer, well over 1100 kilometres to office during this thesis.

Espoo, 2 November, 2015

Niko Heikkinen

Table of Contents

List of Abbreviations

AAS	Atomic Adsorption Spectroscopy
FAAS	Flame Atomic Adsorption Spectroscopy
GC	Gas Chromatography
GC-MS	Gas Chromatography - Mass Spectrometry
GC-PID	Gas Chromatography - Photoionization Detector
GLM	Generalized Linear Model
ICP	Inductively Coupled Plasma Spectrometry
ICP-AES	Inductively Coupled Plasma - Atomic Emission Spectroscopy
ICP-MS	Inductively Coupled Plasma - Mass Spectrometry
ICP-OES	Inductively Coupled Plasma - Optical Emission Spectrometry
TRF	Time-resolved fluorescence
EEM	Excitation-Emission matrix

1 Introduction

1.1 Background

In oil extraction process and numerous other industries, water plays a significant role. With a new oil well, water is present from the very beginning. Although crude oil accounts for the majority of the production volume, towards the end of oil reservoir lifecycle, water-to-oil ratio normally increases considerably, often surpassing the volume of extracted crude oil. The water associated to the oil production process is known as produced water. As a result of the large volumes of produced water, a problem is generated by the produced water salinity, which leads in suitable conditions to scale precipitation and deposit forming on to the metal surface of oil production pipelines.

To address the problem of deposit forming and resulting liquid flow disturbance, scale inhibitors are used in the oil industry. Scale inhibitors are used to prevent the precipitation of common scales, thus avoiding scale accumulation and costly maintenance breaks. Although maintenance brakes have high operational costs, neither is the use of scale inhibitors inexpensive. For this reason, it would be valuable information to know the volume of needed scale inhibitors. To assess the amount of required scale inhibitors, a measurement application to detect the scale causing components would be useful.

Within produced water, scale forms because ions in aqueous solution precipitate when a certain concentration equilibrium is reached. When the equilibrium state is exceeded, the scale potential increases and scale begins to accumulate. In order to assess the scale potential, several traditional analytical techniques exist. Despite the variety of possibilities, generally they need extensive operator knowledge to maintain and calibrate the equipment, as well as interpret the results. In contrast to traditional techniques, this thesis attempts to create an easy-to-use measurement procedure by

using time-resolved fluorescence (TRF) in order to deliver reliable measurement results rapidly.

1.2 Objectives and scope

The experimental problem for this thesis is related to the inherent presence of different scale causing components in produced water. These components are capable of scale formation in produced waters, resulting in an increased scale potential within oil production pipelines. In order to measure the scale potential of produced water, this thesis examines a method of time-resolved fluorescence liquid analysis for detection of calcium, barium and sulphate ions found in produced waters. The resulting method should enable the future development of a measurement application for use in oil production process control. To accomplish this objective, the thesis compares different sensor chemistries used with a time-resolved fluorescence measurement technique to determine ion concentrations in a produced water matrix. The developed methods should be capable of evaluating a large number of possible surface chemistries. The methods are tested with a prediction model that uses the surface chemistries to measure sample ion concentrations.

A measurement procedure requires a reference or standard. With measurements, such as physical quantities, length and mass can be measured directly, however, with chemical quantities, they must be evaluated indirectly. By revealing the latent information with a measurement, the composition can be compared against a known sample. In this thesis, the known sample database is created with synthetic samples, and the field samples are afterwards compared against the synthetic sample measurement data.

Although the practical problem of this thesis is related to an oil production process, the purpose is not to study oil production assurance. Instead, this thesis investigates methods for developing an ion detection platform that can identify and quantify scale components from produced water samples. Thus, it is not only restricted to oil produc-

tion assurance, but also the knowledge can be used in other time-resolved fluorescence molecule detection applications as well.

From the end application point of view, the objective for this thesis was to develop methods to monitor the process flow and detect early possible scaling problems. Therefore, this thesis serves as a preliminary study to examine the potential of a photoluminescence based measurement method that would be able to detect and quantify the scaling components from an oil field process stream.

2 Literature review

This chapter reviews the literature related to produced water and the current methods for analysing produced water samples. In order to gain a comprehensive background knowledge for the experimental part of this thesis, the chapter begins with an introduction to the sample matrix. The sample matrix, or produced water, is discussed in Section 2.1. Section 2.2 describes currently used ion assay methods for produced water samples. Sections 2.3 and 2.4 introduce the principles of photoluminescence measurements used in the experimental part of this thesis.

2.1 Produced water composition

Produced water is a generic name for the water that is pumped up from an oil well during the extraction process. This water consists of two main components: formation water and floodwater. Formation water denotes the water trapped with the oil in a reservoir. Some of the formation water has been within the reservoir as long as the oil itself while some of it has leaked from the surrounding soil into the reservoir. Conversely, floodwater originates from a surface water source. Floodwater is injected from the surface into the reservoir by the well operator. The injection is performed in order to enhance oil recovery by increasing the hydrostatic pressure of an oil reservoir (Dórea et al. 2007, Igunnu & Chen 2014, Fakhru'l-Razi et al. 2009) .

Produced water is a diverse mixture of varying constituents. The composition of produced water is a result of the complex geological environment from which it is gathered (Røe Utvik 1999). Furthermore, produced water is a mixture widely varying water sources which become combined with other soil-originating substances (Boitsov et al. 2004). In addition, it is not rare that several oil wells are connected together through pipelines, thus producing combination streams of different brine sources.

As the demand for oil is hardly diminishing in the near future, the need for enhancing reservoir yield requires better monitoring methods. In these situations, the knowledge

about produced water becomes increasingly valuable. From total oil production volume, produced water can exceed hydrocarbons in great extent; moreover, as the oil well matures, the amount of produced water tends to increase (Kelland 2014). At the end of the well lifecycle, produced water volume can increase up to 98% of the total production stream (Ray & Engelhart 1992, Røe Utvik 1999) . Figure 1 illustrates a typical oil well production profile regarding the oil and produced water yield. With increasing extracted water-to-oil ratio, scaling may cause major process problems. Therefore, knowing the produced water composition is important information for the well operator.

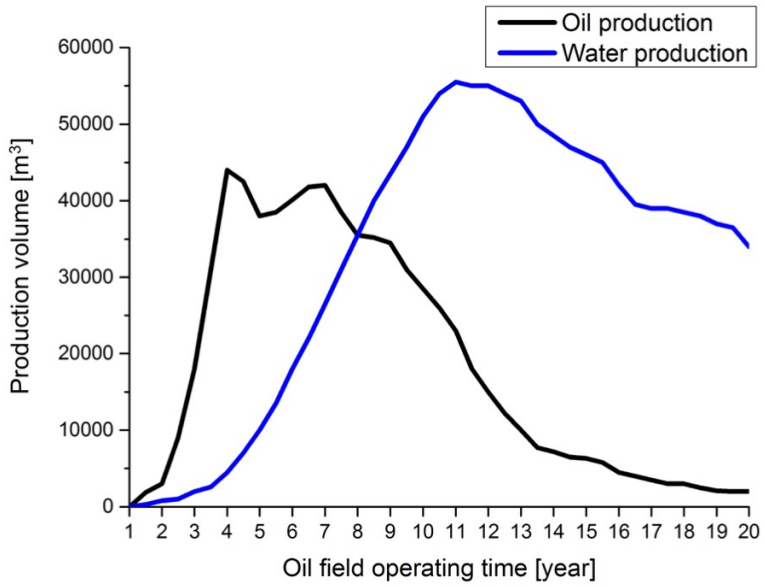

Figure 1 - Typical production profile for oil and produced water (Igunnu & Chen 2014)

Because of the diverse geographical environments from which produced water samples are collected, the composition varies from location to location and even within the same location during a well lifecycle. In addition to a single origin for produced water, oil wells are usually distributed throughout the whole oil field. This distribution creates additional variability to the produced water by combining several brine sources within production pipelines (Kelland 2014).

Produced water composition can be divided into four categories: organic constituents, inorganic constituents naturally present components, and those chemical compounds

added by the well operator to ensure process flow (Igunnu & Chen 2014) . The naturally present organic and inorganic constituents consist of

- dissolved and dispersed oil and grease
- heavy metals (Cd, Cr, Cu, Pb, Ni, Ag, Zn)
- radionuclides (^{226}Ra, ^{228}Ra) (Veil et al. 2004, Igunnu & Chen 2014, Ray & Engelhart 1992) .

In addition to the naturally present constituents, oil extraction requires flow assurance chemicals for purposes, such as scale forming prevention and enhanced water-oil separation (Igunnu & Chen 2014) . These added chemicals may consist of the following molecular components:

- corrosion inhibitors
- oxygen scavengers
- scale inhibitors
- biocides
- emulsion breakers and reverse emulsion breakers
- coagulants, flocculants, clarifiers
- solvents (Veil et al. 2004, Kelland 2014, Ray & Engelhart 1992) .

Moreover, oil extraction process stream may include waxes, dissolved gases and microorganisms (Veil et al. 2004, Igunnu & Chen 2014, Ray & Engelhart 1992). Thus, the chemical composition of produced water is rather complex, mainly as a result of the possible components present but also because of the varying component concentrations. Table 1 presents the variability in produced water component concentrations in several geographical locations.

Table 1 – Scale inducing ion concentrations in different geographical locations (Alzahrani & Mohammad 2014, Dórea et al. 2007, Igunnu et al. 2007)

Reference	Alzahrani & Mohammad 2014, p.123		Dórea et al. 2007, p. 237		Igunnu et al. 2007, p.159	
Well location	Several locations		North Sea		Several locations	
Component	**Concentration (ppm)**		**Concentration (ppm)**		**Concentration (ppm)**	
	Min	**Max**	**Min**	**Max**	**Min**	**Max**
Ba^{2+}	0,07	468	-	-	1,3	650
SO_4^{2-}	<1	15 000	-	-	<2	1650
Ca^{2+}	<1	74 185	-	-	13	25 800
Cu^{2+}	-	-	0,001	0,001	<0,02	1,5
Fe^{2+}	0,1	4770	4310	4770	<0,1	100
Cr^{3+}	-	-	-	-	0,02	1,1
Cl^-	<1	254 923	16 100	19 500	80	200 000
Na^+	<1	149 836	8800	9600	-	-
CO_3^{2-}	7,3	1030	-	-	-	-

Although the produced water has a high diversity of constituents, the main components of this thesis were limited to those that cause scale in a process equipment. The main components for scale forming in oil production are

- calcium carbonate
- sulphate salts (Ca, Ba, Sr, Fe)
- sulfide scales
- sodium chloride (Kelland 2014, Veil et al. 2004).

As explained in this section, the composition of produced water has many factors that alter the sample matrix. A sample matrix in this thesis denotes for the solution in where the analyte (calcium, barium or sulphate) is delivered to the measurement. Therefore, although it is important to identify the matrix composition, more important is to select sensor chemistries that are mainly selective to the analyte entities, thus they are providing information about the analyte regardless of the matrix constituent variability. Sensor chemistry denotes for the components that interact with the sample analyte in order to produce a measurement signal output. Sensor chemistries are further discussed in Section 2.4.

2.2 Current produced water analysis methods

Analytical techniques related to scale formation component analysis studied in this literature review are mainly based on inductively coupled plasma (ICP), gas chromatography (GC) and atomic adsorption (AAS) spectroscopic applications. In general, the literature related to scale component detection is focusing on the environmental discharge assessment of produced water (Dórea et al. 2007, Røe Utvik 1999, Boitsov et al. 2004, Bezerra et al. 2007). Thus, these studies are discussing the topic of produced water composition in wider perspective. The main focus with these studies is in hydrocarbon compounds rather than merely in scale causing components. In the literature (Fakhru'l-Razi et al. 2009, Dórea et al. 2007, Røe Utvik 1999), the component analyses are performed with the following measurement techniques:

- Gas Chromatography - Mass Spectrometry (GC-MS)
- Gas Chromatography - Photoionization Detector (GC-PID)
- Atomic Adsorption Spectroscopy (AAS)
- Flame Atomic Adsorption Spectroscopy (FAAS)
- Inductively Coupled Plasma - Atomic Emission Spectroscopy ICP-AES)
- Inductively Coupled Plasma - Mass Spectrometry (ICP-MS)
- Inductively Coupled Plasma - Optical Emission Spectrometry (ICP-OES).

By studying the literature related to the current methods revealed information about the sample matrix as well as the techniques relevant to the industry for analysing components from produced water samples. This literature survey indicated that photoluminescence based methods were not widely used for ion detection from produced water samples. In this perspective, this thesis could extend well-studied TRF-techniques (described in Section 2.3 and 2.4) to provide a novel measurement solution for produced water analysis.

As for the comparative study against the developed photoluminescence based method, according to the literature, an ICP-OES method was found to be widely used in the oil production industry for determining alkaline earth metal constituents from produced water samples.

2.3 Time-resolved fluorescence background and measurements

Time-resolved fluorescence (TRF) was selected for the measurement method because of its suitability for creating an easy-to-use measurement platform that can deliver reliable measurement results rapidly (Hänninen et al. 2013). To achieve the objectives of this thesis was to experimentally determined suitable conditions and environment for time-resolved fluorescence measurement for given sample analytes.

In order to reveal information from a target molecule, a pulsed light is used at TRF measurement to excite electrons from a ground state to an excited state. After the electrons of a sample molecule have been excited, the gained energy is released in several different ways. The energy is released either by dissipation to the surrounding environment or with the following competitive processes:

- fluorescence photon emission
- nonradiative dissipation (heat)
- energy transfer to neighbouring molecules
- transfer to a lower excited state (an excited triple state) (Albani 2007) .

A schematic Figure 2 illustrates the energy transfer mechanisms related to photoluminescence. In this thesis, the main component for creating the photoluminescence reaction was a luminescent Europium(III) 2,2’:6’,2”-terpyridine derivative chelate (Mukkala et al. 1993), which was used to extract time-resolved photoluminescence response from a sample.

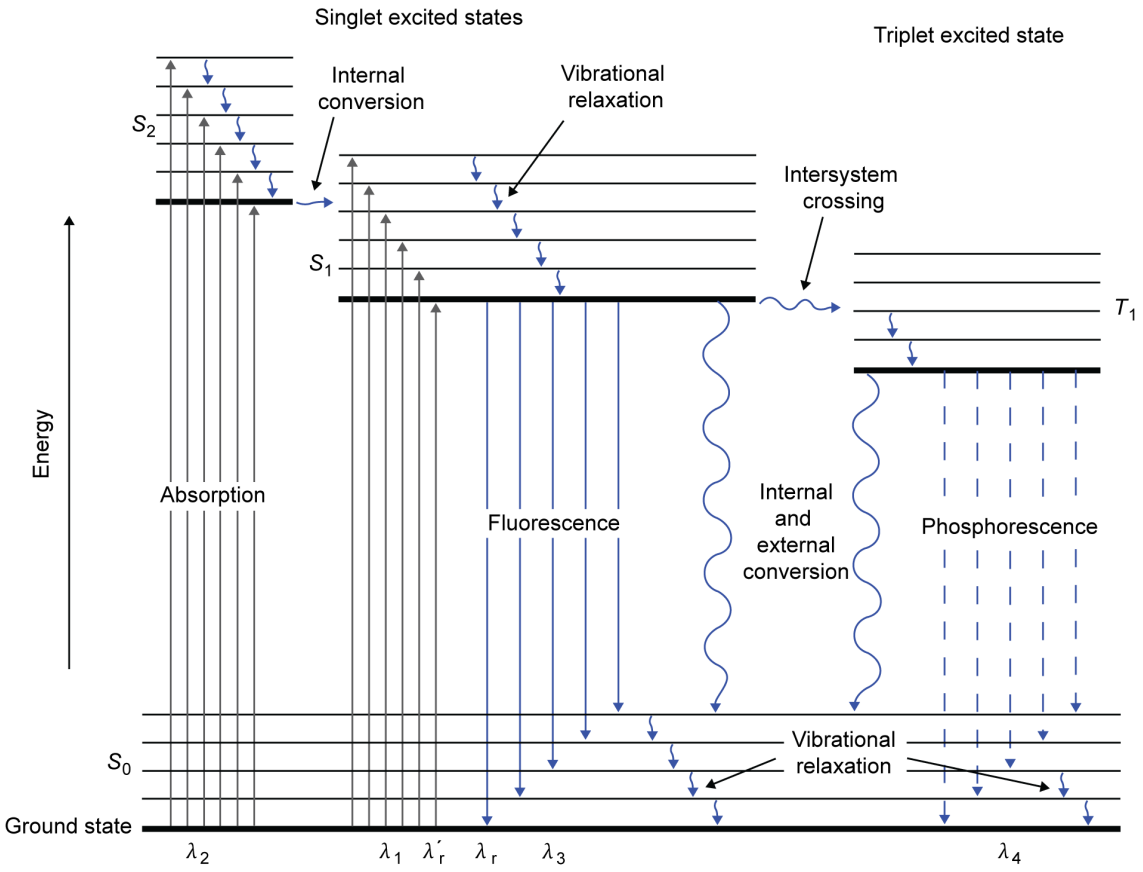

Figure 2 - Partial energy-level diagram for photoluminescent system (Skoog 2007, p. 401)

Fluorophores, organic structures capable for photoluminescence, are very diverse group. For example, aromatic hydrocarbons in produced water present these properties (Lee & Neff 2011). As a result of this abundantly present ability among molecular entities, it is difficult to extract information from a specific photoluminescence spectrum without time-resolved fluorescence. If time-gated measurement is not used, the background noise will mask relevant spectral information about the analyte under examination (Siivonen et al. 2014). According to Yang & Wang (2005) the background noise can be divided into three categories: sample autofluorescence, light scattering (Tyndall, Rayleigh or Raman), and equipment luminescence properties (created by cuvettes, filters or lenses). Therefore, a method is needed to separate interference from relevant information.

A solution to this problem is the photoluminence properties of lanthanides. With a long-lived luminescence and wide excitation-emission Stokes' shift, most of the background interference is removed by starting the actual measurement after disturbing

fluorophores have been extinguished (Figure 3). Figure 3 is presenting the time-resolved fluorescence measurement cycle, where the pulsed ultraviolet light is exciting the analyte-chelate entities and the signal starts to decrease as a function of time (Dickson et al. 1995, p.8) . After a predetermined “delay time” or “lag time”, most of the background interference has extinguished and during the “measuring time” or “integration time”, the photoluminescence emission signal is recorded with a photomultiplier tube (PMT). Generally, the measurement cycle is repeated several consecutive times, thus enhancing the signal to noise ratio (Yuan & Wang . 2005, p.560).

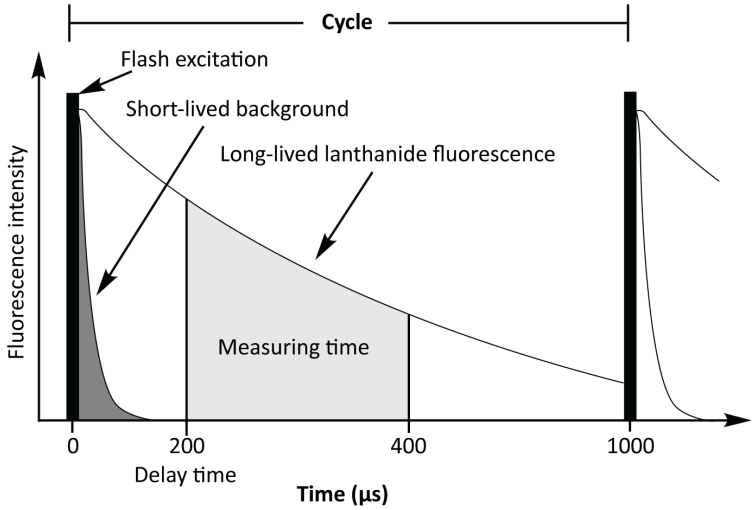

Figure 3 – Pulsed measurement cycle in time-resolved fluorescence (Yuan & Wang 2005, p.560)

As a result of time-gated measurement, dynamic range and sensitivity can be enhanced significantly (Hagan & Zuchner 2011) . Typical excitation and emission wavelengths for lanthanide complexes used in life-science assays are in 320–360 nm and 615 nm respectively. This however, is not the situation with plain lanthanide ions, since they have low quantum yield. In order to gain a photoluminescence signal from lanthanides, they need a ligand “antenna”. In this process, the ligand chelates with the lanthanide ion, resulting in a Ln-complex that absorb electromagnetic radiation with the ligand structure and emit the gained energy through the lanthanide ion (Dickson et al. 1995, p.6) .

As a result of the lanthanide complex energy absorption, transfer and release properties, a large Stokes' shift is achieved. Since the excitation of the chelate is not creating interference to the emission spectrum, the separated Stoke's shift (Figure 4) enables better sensitivity of the fluorescence measurement (Siivonen et al. 2014). The combination of time-gated measurement and large stokes' shift create a suitable measurement environment to separate efficiently relevant spectral information from background noise and interference.

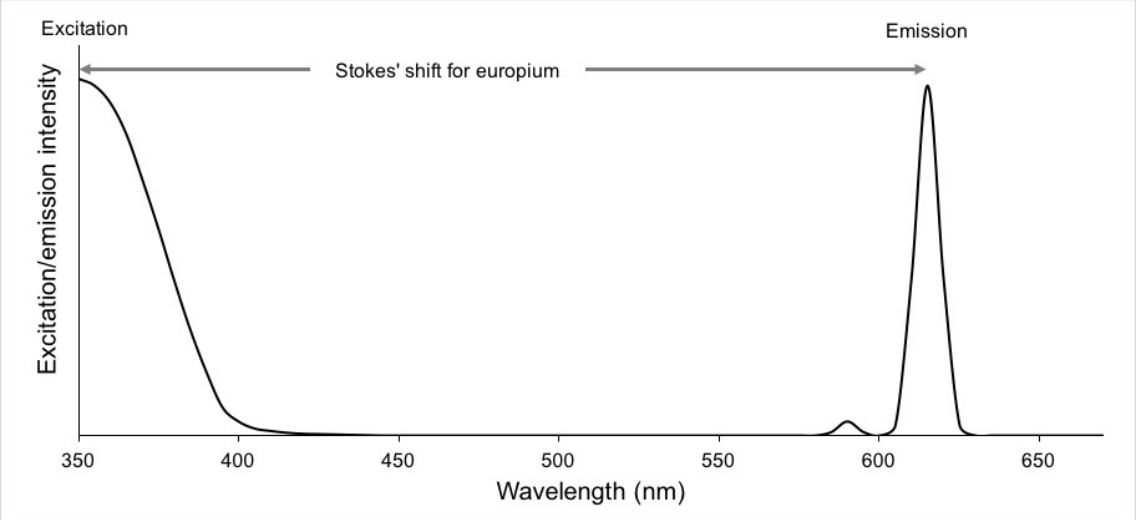

Figure 4 - Europium [Eu^{3+}] Stokes' shift (PerkinElmer Inc. 2015)

In TRF measurement, the chelate is combined with a sample solution in order to create measurement environment. In addition to the combination of chelate and sample, a signal alternating component is needed to create separation between the reference and added ion sample (Table 2). Figure 5 is presenting a schematic illustration of the created TRF measurement environment, which include specific and non-specific interactions for producing difference in the emission signal between the reference and analyte sample (Hänninen et al. 2013, Anzenbacher et al. 2010) .

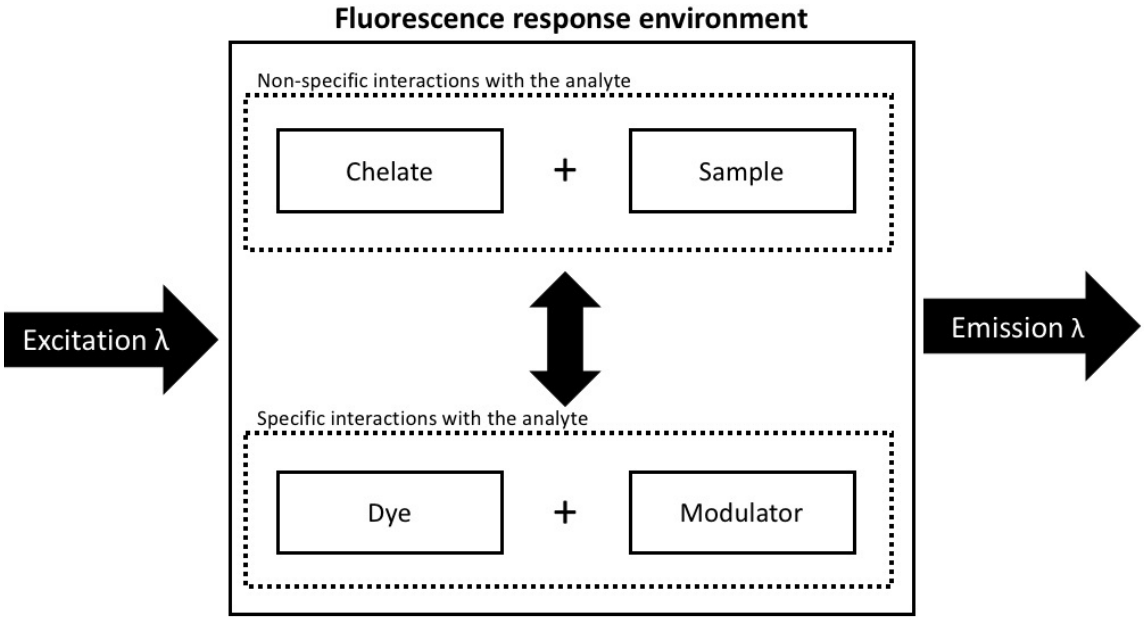

Figure 5 - A schematic illustration of the excitation-emission signal alteration environment

In Figure 5, the chelate is first combined with a sample and then the resulting solution is combined with a ionochromic dye-modulator solution. In this thesis, a sensor element is either an ionochromic dye alone or a combination of ionochromic dye and an ion binding molecule (modulator). As a result, specific and non-specific interactions between solution components produce an altered signal output that can be used to detect specific ion from a given sample. The ion evaluation is conducted by using known samples (a calibration data set) to interpret the signal output from the photoluminescence emission signal seen at Figure 5.

Table 2 - Example measurement results with and without dye-modulator component

Added ion [Ca^{2+}] concentration (mg/dm^3)	**Chelate + Dye-modulator (B4) signal**	**Chelate signal**
500	39 744	168 814
250	54 922	165 447
100	74 012	165 371
50	94 157	164 043
5	123 411	167 211
1	145 804	163 238

B4 = a dye-modulator sensor defined at Appendix 3

Table 2 present measurement results from an experiment where the same sample is measured with two different surface chemistries. In this experiment, an added ion sample was diluted as described in the concentration column and two measurements were conducted with and without a dye-modulator. As can be seen from the measurement results (Table 2), although the added dye-modulator is quenching the signal level, a separation between the concentrations become explicit, whereas without dye-modulator, the output signal remains relatively unchanged. The same behaviour was reported also by Siivonen et al. (2014)

2.4 Fluorescence fingerprint sensors

In this thesis, a term sensor is denoting for all entities that produce a signal response in the TRF-measurement. Anzenbacher et al. (2010) defined a chemical sensor as a device that responds to a particular analyte, however in this thesis, the relationship between the sensor and analyte is hardly specific to a single analyte entity. A better description is that the sensors are interacting with the analyte ions with cross-reactivity. Cross-reactivity (non-specificity) connotes for the sensitivity to other substances in addition to the analyte molecules (Hänninen et al. 2013). When developing a photoluminescence measurement system based on cross-reactive sensors, the resulting system needs several sensors to identify the target analyte.

The principles of assay methodologies are described by Hänninen et al. (2013) and Anzenbacher et al. (2010), in where a certain set of chemical sensors can be used to fingerprint desired sample matrices. After the response ”fingerprint patterns” have been recorded, the analyte entities can be identified by comparing the measurement results to the fingerprint library attained from the known sample measurements. The functionality and response behaviour of a chemical sensor is derived from two structural properties known as receptor and transducer moieties. With these moieties, the sensor is able to interact physically or chemically with the target analyte and produce a modified signal output. In most cases, the analyte interaction and selectivity is related to the receptor moiety and the output signal response to the transducer moiety (An-

zenbacher et al. 2010). In this thesis, the output signal is interpreted as a photoluminescence signal (photons received by the PMT-transducer).

Although the produced water composition can vary greatly, according to the literature, it is possible to create a photoluminescence-based measurement method that would fulfil the requirements determined in the objectives and scope of this thesis. The knowledge built upon the literature and with carefully selected surface chemistries, the identification of the scale causing components should be possible. The resulting ion detection method or water fingerprinting application development is discussed at the following chapters.

3 Experimental part I

The experimental part of this thesis is divided into two parts. Experimental part I addresses the problem how to select sensors for the detection of Ba^{2+}, SO_4^{2-} and Ca^{2+} ions. Experimental part II explains how these selected sensors can be used to analyse produced water samples.

The experimental objective for this thesis is to develop a photoluminescence-based liquid fingerprinting application. A unique sample fingerprint can be created by analysing excitation-emission light interactions between a sample and surface chemistry. This unique sample fingerprint can be used to determine analyte entities from a sample liquid. In this thesis, these analyte entities represent the different scale causing components in an oil production process. In the oil production process, apart from corrosion and gas hydrates, pipe scaling forms one of the most serious problems in the oil production process; in the worst case scenario, scale can accumulate onto the pipe surface and halt the production flow within 24 hours if the scaling problem is not addressed accordingly (Kelland 2014).

Because pipe scaling can develop at such a rapid pace and disturb oil production flow, the current analytical methods fail to resolve the problem promptly. Although current techniques enable separate detection of scaling components in minute concentrations (ng dm^{-3}), they are rather laborious (Boitsov et al. 2004). In most cases, samples have to be sent from a field of operations to an off-site laboratory, thus the delay for measurement results can stretch to days. In addition current analytical off-site methods, such as ICP-OES and GC-MS (Røe Utvik 1999), need special expertise to calibrate and maintain the measurement equipment as well as carry out the measurements.

Compared to current methods the approach described here is completely novel. The approach developed in this thesis is based on array of non-specifically interacting sensor elements from which the measured signals are analysed by computer-assisted data analysis. With traditional methods, such as gravimetric titration, the occurring reac-

tions are highly specific. The method described here is based on creating a sample specific fingerprint with a cross-reactive array of chemistries. Fingerprint can be analysed by comparing it against a library of known samples.

The experimental measurements were conducted by using Tecan Infinite M1000 PRO - microplate reader (Tecan Austria GmbH; Grödig/Salzburg; Austria) and 96-well transparent microplate (C96 Maxisorp Nunc-Immuno Plate, Thermo Fisher Scientific). The target for the time-resolved fluorescence measurements were to study the response of different assay components and how they are producing different signal response. Further studies and the second part of this thesis was to use the same methods to measure complex synthetic samples and evaluate the sample composition with the knowledge acquired from the synthetic sample measurements.

3.1 Measurement protocol design

The measurement protocol design was the very first phase of this thesis. The measurement protocol describes all the steps to perform the experimental measurements and therefore it was a crucial part for achieving comparable measurement results between different samples. In general, the protocol describes all of the needed preparation steps and the parameters for the actual measurements.

The measurement protocol can be divided into two parts. These parts are measurement preparation steps and the parameters for the actual TRF measurement. The preparations steps can be further on divided into subcategories, such as: sample, chelate and sensor preparation. Sample preparation describes how to produce the synthetic brine that was used as a reference sample and as a base matrix for the added ion samples. Table 3 lists the used base brine composition. The brine described at Table 3 is a synthetic replicate of produced water based on North Sea oil field produced water.

Table 3 - The composition of brine used for the reference sample and added ion sample matrix

Reagent	Molar mass (g/mol)	Mass concentration (g/l)	Concentration (mmol/l)
NaCl	58,44	35,03	599,00
CaCl2 * 2H2O	147,01	2,24	15,24
MgCl2 * 6H2O	203,30	1,46	7,18
KCl	74,55	0,21	2,82
BaCl2 * 2H2O	244,26	0,13	0,53

As the reference sample in the measurements had a brine composition described in Table 3, the samples with added ion were also produced to the same reference brine. This made it possible to track only the changes caused by the addition of specific ion into the brine solution. The added ion concentration in synthetic samples was 500 ppm.

3.1.1 Microplate preparation

All measurements were conducted with the Tecan Infinite M1000 PRO microplate reader and 96-well transparent microplate (Picture 1). Picture 1 presents an example of plate component arrangement used for the preliminary sensor screening.

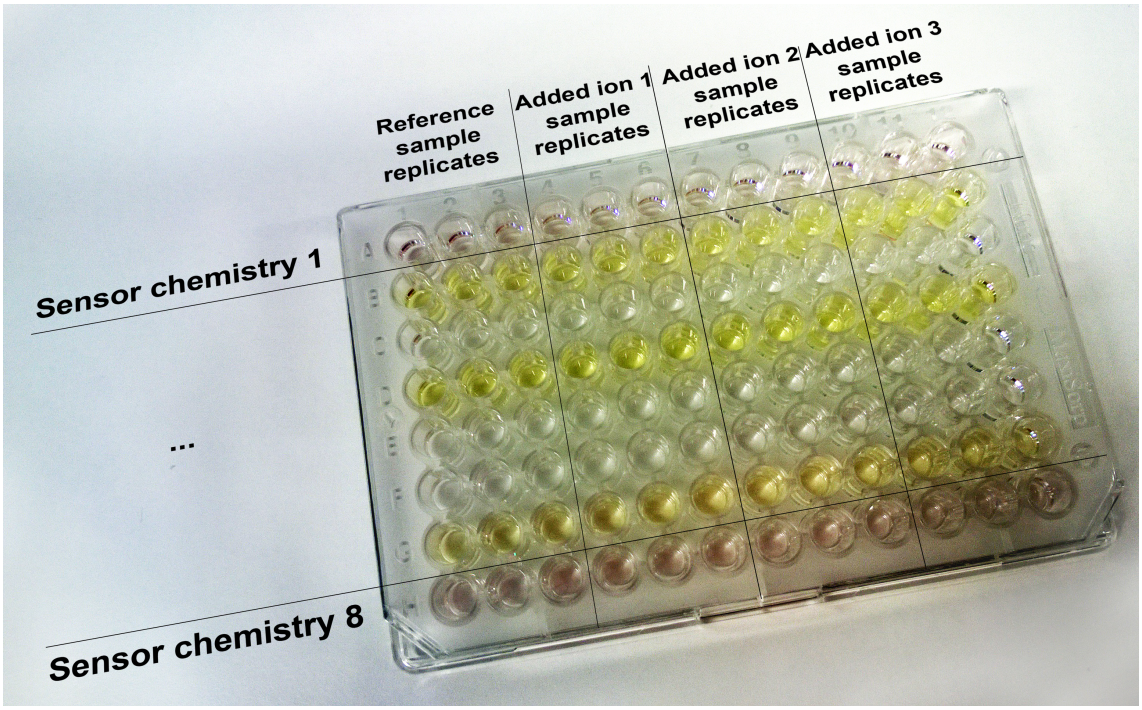

Picture 1 - Sensor arrangement on microplate

The plate components used in this project consisted of:

- ligand-lanthanide chelate
- sensor (Appendix 3)
- sample.

Table 4 presents the component concentrations in a single microplate well. The concentrations in Table 4 were used in the final measurement to evaluate produced water samples. All reagents used in this thesis were analytical quality Sigma-Aldrich products. Appendix 3 lists the different reagents that were used to produce sensors described in Table 5. Appendix 5 lists all reagents used in this thesis with a batch/LOT identification code, CAS number and Sigma-Aldrich identification number.

Table 4 - Microplate component volumes and concentrations for a single well

			Sensor	
	Sample	**Chelate**	**Ionochromic dye**	**Modulator**
Concentration / well (ppm)	0–500	-	-	10
Concentration / well (molarity)	-	0,67 nM	10 µM / 20 µM	-
Volume / well (µl)	100		20	

The microplate preparation procedure was conducted in two steps in which the sensor (ionochromic dye and modulator) solution was first pipetted into a microplate well (20 µl) and after this, the sample-chelate solution was added to the plate well (100 µl). Therefore, two solutions were prepared before mixing all of the components together within the plate well. These components were the sample-chelate and ionochromic dye-modulator solutions. All other components had a fixed concentration except ionochromic dye component, which had two concentrations: 10 µM and 20 µM.

At Table 5, for each ionochromic dye, a set of four different sensor solutions were prepared. The solutions listed at the table were further diluted in the plate well after the addition of sample-chelate solution.

Table 5 - Sensor preparation

ID = ionochromic dye
V_2 = Sensor total volume (µl)
A15 and A16 = modulators defined at Appendix 5

Sensor solution 1

Component (C_1)	**Component (C_2)**	**Dilution factor (D) [C_1/C_2]**	**Needed component volume µl (V_1)**	**Plate well concentration**
ID 10 mM	0,06 mM	166,67	V_2 / D	10 µM
MQ Water			$V_2 - V_1$	

Sensor solution 2

Component (C_1)	**Component (C_2)**	**Dilution factor (D) [C_1/C_2]**	**Needed component volume µl (V_1)**	**Plate well concentration**
ID 10 mM	0,12 mM	83,33	V_2 / D	20 µM
MQ Water			$V_2 - V_1$	

Sensor solution 1 + 2nd component

Component (C_1)	**Component (C_2)**	**Dilution factor (D) [C_1/C_2]**	**Needed component volume µl (V_{1n})**	**Plate well concentration**
ID 10 mM	0,06 mM	166,67	V_2 / D = V_{11}	10 µM
Modulator 1000 ppm [A15 or A16]	60 ppm	16,67	V_2 / D = V_{12}	10 ppm
MQ Water			$V_2 - (V_{11} + V_{12})$	

Sensor solution 2 + 2nd component

Component (C_1)	**Component (C_2)**	**Dilution factor (D) [C_1/C_2]**	**Needed component volume µl (V_{1n})**	**Plate well concentration**
ID 10 mM	0,12 mM	83,33	V_2 / D = V_{11}	10 µM
Modulator 1000 ppm [A15 or A16]	60 ppm	16,67	V_2 / D = V_{12}	10 ppm
MQ Water			$V_2 - (V_{11} + V_{12})$	

3.1.2 Measurement parameters

Table 6 specifies the parameters for Tecan Infinite M1000 PRO time-resolved fluorescence measurement. The given parameters were used to measure microplates described at the earlier Section 3.1.1.

Table 6 - Tecan Infinite M1000 PRO measurement parameters

Used settings	Description
Excitation wavelength 230–400 nm, Bandwidth 10 nm **Emission wavelength** 580–635 nm, Bandwidth 6 nm Sensor specific wavelengths presented at Appendix 3	Bandwidth is defined as Full Width at Half Maximum intensity (FWHM)
Flash cycles 100 Hz, counts 60–100	Xe-Flash lamp frequency and the number of flash cycles
Mode Top	Measurement conducted from above the plate
Gain 200-255	The sensitivity of photo-multiplier tube (PMT)
Z-Position 20150 µm	The distance of excitation lamp to the plate well
TRF settings Lag time: 200 µs Integration time: 400 µs	Time-resolved fluorescence settings

The values given at Table 6 are representing a set of parameters for the entire experimental part I. These parameters were used to analyse sensor chemistries at preliminary stages. As the number of sensors were reduced during the experimental part I, also the measurement parameters narrowed down. The final parameters are presented at Appendix 3, where each sensor has a specific wavelength for performing the measurement.

3.2 Sensor evaluation

The task in the experimental part I was to study altogether 112 sensors with 216 different excitation-emission wavelength pairs. First of all, the purpose of this phase was to evaluate and select sensors that can separate reference and added ion samples, and secondly, determine what wavelengths are suitable for each sensor. Excitation-emission matrices for a single sensor with 216 different wavelengths are presented at Picture 2. At Picture 2, the vertical axis column denotes for the excitation wavelengths and horizontal axis the corresponding emission wavelengths. The signal values presented in the matrix cells are the measured signals in the given excitation-emission wavelength. The task was to compare each produced matrix cells (measured signals)

between the reference and added ion sample, hence, detect the wavelengths that are producing a difference between the measured signal values.

Brine reference sample

Ex/Em	580	585	590	595	600	605	610	615	620	625	630	635
230	-2208	-2462	35357	12127	11177	24932	24203	10555	525	-16659	7372	-9183
240	-798	-6490	3836	8016	16757	12183	5392	38254	43565	10757	14321	8776
250	8830	578										
260	6103	831										
270	1600	1128										
280	10274	1883										
290	764134	74781										
300	17614	4391										
310	17978	2888										
320	9000	2814										
330	6841	2608										
340	12926	2452										
350	3653	1598										
360	6327	532										
370	3631	351										
380	-706	-1										
390	-1962	73										
400	252	17										

Added ion sample

Ex/Em	580	585	590	595	600	605	610	615	620	625	630	635
230	30115	-423	13957	-13064	42770	6173	16237	6216	44904	50266	-7524	3982
240	-1668	15518	-3389	26040	9608	4034	21348	61805	34282	16884	-693	9570
250	3512	4557	9790	20401	9866	7038	12642	28377	34490	5714	943	11907
260	5327	4939	17795	22600	9646	8985	17177	37301	31929	17081	14616	-2060
270	6309	8442	17209	19242	15677	7283	20278	47755	59652	19846	4517	10578
280	6231	20539	25018	24431	25314	13712	31406	55801	70806	21608	5155	10846
290	736916	673058	280625	75317	52585	12595	41073	86581	104109	53806	10972	7462
300	21624	39315	176293	455412	670803	15025	50592	114915	103544	55341	21151	17742
310	16018	24292	28086	32542	34237	12488	55099	103257	95807	36377	19343	3177
320	13545	25511	33963	57502	30547	9816	43037	104274	103617	36027	11967	5495
330	12623	22967	42836	49970	39320	18519	47914	92326	118044	60752	15936	9233
340	9480	17590	31861	43064	26330	9800	35284	105423	95487	38297	17273	4735
350	8051	9293	16457	27705	19848	11175	29339	60724	61072	25206	12666	8594
360	3717	2976	4375	7357	5799	4913	6154	18822	13627	7261	2018	4402
370	1191	5557	3424	519	4594	1737	2716	699	6625	637	-772	510
380	1602	1088	3834	1577	3491	3805	7676	3930	3823	5768	3180	180
390	-461	-693	2650	2848	1186	-286	4373	4961	3041	-590	1045	-3548
400	446	500	2507	2713	841	3283	3016	1564	306	-1553	821	4338

Picture 2 – Excitation-emission matrices (EEM) for reference sample and added ion sample

As a result of having 112 sensors with 216 different excitation-emission wavelength pairs, the screening array had 24 192 individual sensor combinations. In addition, as a single screening array consisted of a reference sample and three different added ion samples, the number of individual data points for a single measurement was 96 768, without any replicates. Therefore, the assessment of excitation-emission matrix (EEM) data was not possible without automation. The solution for this problem was to create a data handling algorithm (Appendix 1) that detect relevant information from the raw data and illustrate this information in a reduced format.

As can be examined from Picture 2, finding relevant changes from EEMs is rather cumbersome task and therefore a R-algorithm (R Core Team, 2015) was written to evaluate the changes between several EEMs and presenting the relevant separation information in a graphical form. Picture 3 presents 3D surface plots from the same EEMs as presented at Picture 2. From these surface plots it is possible to illustrate the main problems present with the measured raw data.

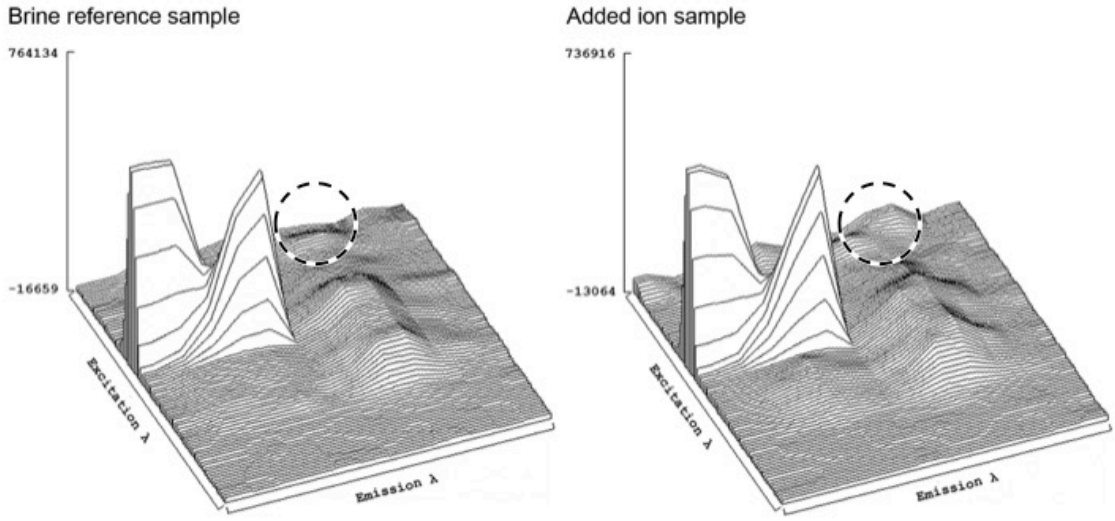

Picture 3 – Excitation-emission matrix 3D surface plots

In measurement raw data, the main problem is the high signal level peaks that are concealing the small signal level changes. This is problematic because a small absolute signal difference in low signal level might be as significant as a large absolute difference at high signal level. An example from this kind of excitation-emission area is highlighted with a dashed line at Picture 3. Moreover, problematic is the signal range produced by the measurement device (Tecan Infinite M1000 PRO) that can be starting from negative values and continue to signal maximum photon counts. The negative values are produced by an automatic blank reduction feature of the measurement device.

In order to summarise the sensor evaluation phase, the problem about the measurement data analysis was mainly related to the amount of raw data, which was too large to be evaluated by hand. This evaluation would have been excessively time consuming, therefore, it was imperative to design an automatic data handling algorithm for performing most of the preliminary screening data analysis.

3.2.1 Data handling methods for preliminary sensor screening

Because of the data handling problems described in the previous sections, a data-handling algorithm was produced to evaluate relevant signal differences and thus reduce the data obtained from the TRF measurements. The purpose of this algorithm

was to produce a graphical presentation of the relevant signal differences, where the small changes in the low signal levels were not concealed by the high signal level values. Appendix 1 describes the algorithm in detail with a flow chart.

The most important part of the algorithm was the low-high signal level comparison method. As presented at Table 7, the problem of low and high signal differences was solved by using a logarithm transformation function (Equation 1).

Equation 1

$$X' = log(x+1)^{4.67}$$

, where X' is the logarithmic transformed matrix cell value
x is the original matrix cell value.

The power 4.67 given in the Equation 1 is a modification factor that fits the logarithmic function to the desired form. The desired function form equalized the low signal level changes to the high signal level changes in right proportions. Table 6 presents an example of how signal separation in different ranges should be compared.

Table 7 - Assignment of signal difference correspondence

Reference sample signal (A)	**Added ion sample signal** (B)	**Original signal remainder** (A-B)	**Log transform (A)** [log(A+1)^4,67]	**Log transform (B)** [log(B+1)^4,67]	**Transformed signal remainder**
4 973	6 000	**1 027**	464	514	**50**
46 077	50 000	**3 923**	1 380	1 430	**50**
93 733	100 000	**6 267**	1 864	1 914	**50**
772 605	800 000	**27 395**	4 124	4 174	**50**

At Table 7, the signal remainders of a reference sample and an added ion sample are assessed against the values transformed with Equation 1. From Table 7, it can be seen that after the transformation, the signal log remainders were comparable. Therefore, it was possible to evaluate and compare reference and added ion sample signal differences throughout the whole signal range.

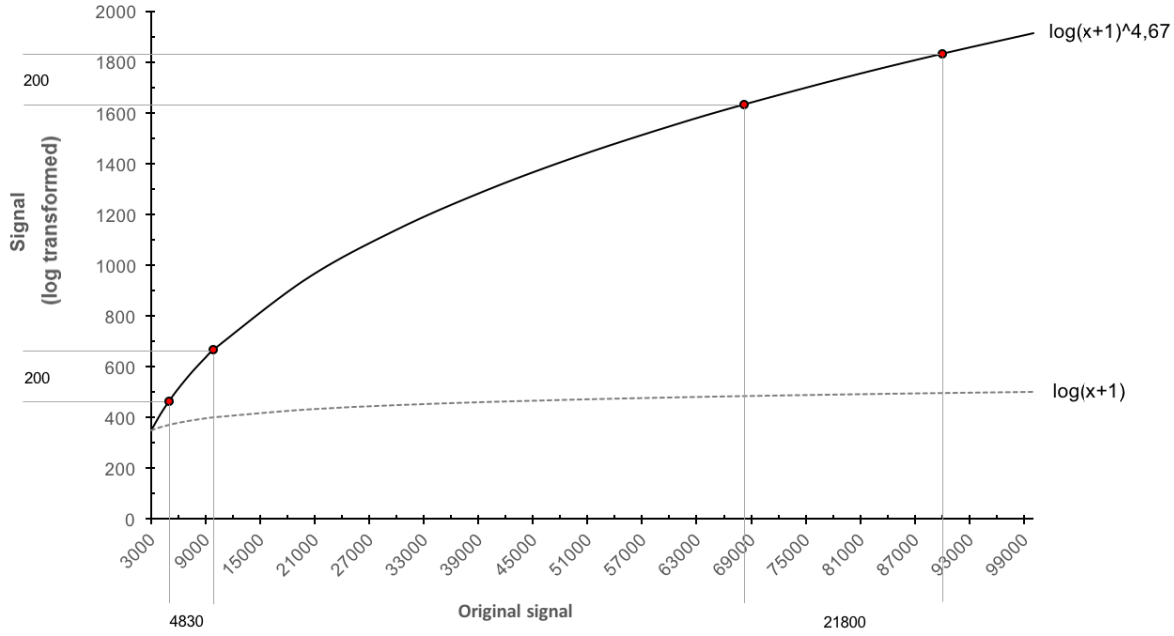

Figure 6 - Logarithmic function for signal difference evaluation

The logarithmic transformation function depicted in Figure 6, illustrates the log transformation curve (solid line) and how the original matrix cell values are transformed into logarithmic values. These transformed remainder values can be compared through the signal range. In addition to the transformation function (Equation 1), Figure 6 presents a function curve without a power modification factor. As can be seen from this curve, the function modification factor is needed to fit the transformation function into a form that is able to compare signal differences in a meaningful matter. Without the modification factor, the curve would plateau, thus producing an opposite situation compared to the initial problem; the low signal level values would conceal the high signal level separation values.

Figure 6 presents the algorithm transformation space, where the x-axis illustrates the original signal values and the y-axis the transformed logarithmic values. As can be seen, the signal values less than 3000 were omitted in order to remove bias from the instrument noise. Therefore, the algorithm was using only relevant values in transformation process.

In order to assess the added ion sample differential against the reference sample, a R-algorithm was used to produce an illustration of the differential responses. The final

illustration is presented later in this section; Figure 7 is explaining the rationale behind the differential plots presented later at Figure 8.

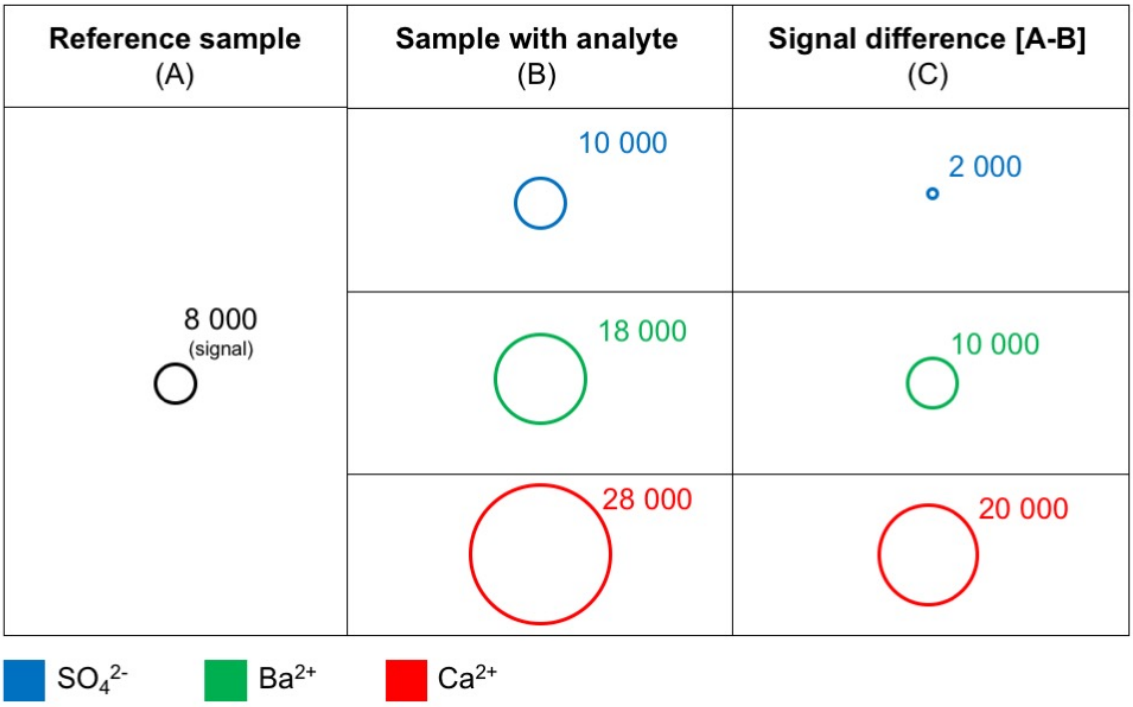

Figure 7 – Visual sensor evaluation of signal differences between three different ions

In Figure 7, arbitrary signal values are used to explain how a signal difference between a reference sample (A) and an analyte sample (B) is created. The resulting signal difference circle (C) describes how well a certain sensor chemistry is separating the reference and analyte sample. At Figure 7, the signal separation (C) is the remainder of values A and B. In addition to the smallest separation circle (blue), related to signal difference for SO_4^{2-}, several circles can be examined at the same time. In Figure 7, the green circle is depicting the separation for barium and red circle calcium. With this visual presentation, it was possible to evaluate sensor responses for each ion. Even without the exact numerical values given in Figure 7, conclusions can be made about the sensor functionality and behaviour. The use of this method enabled the simultaneous examination of each sensor response to various analytes.

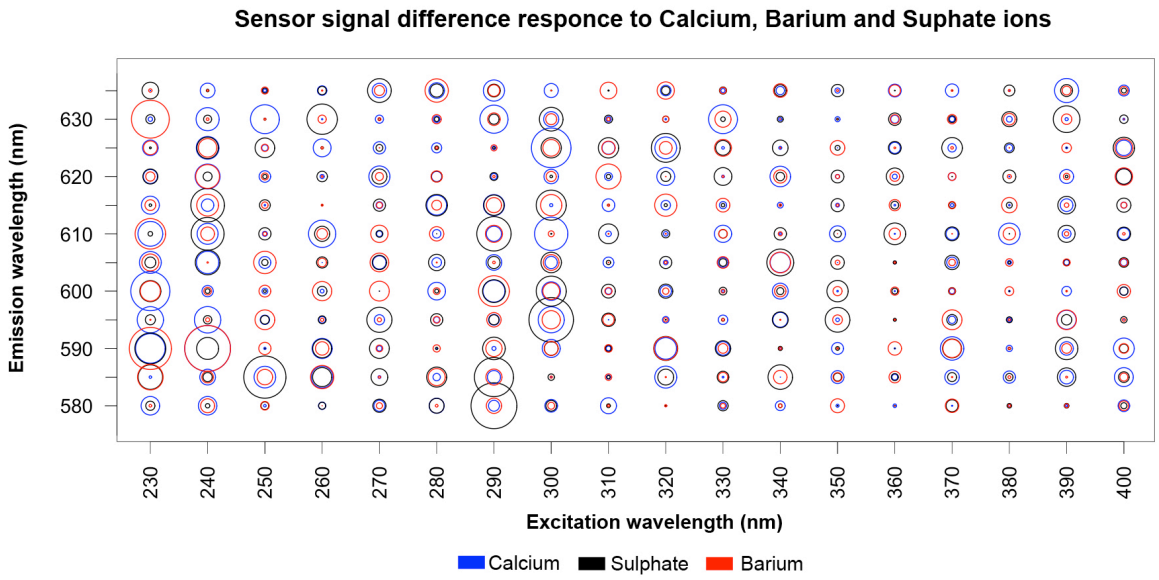

Figure 8 - R-algorithm difference plot for a modulator

The sensor evaluation method is illustrated in Figure 8, where each excitation-emission wavelength is connected to the separation of reference and added ion for a single sensor. By using the given figure, it was possible to evaluate how well a sensor was separating reference and added ion samples, as well as determine in what wavelength area. The comparison of the figures for different sensors enabled the determination of sensors that were sensitive to the analyte entities. Therefore, this method was the main tool for reducing the data from the preliminary sensor screening and assess the most suitable sensors for further studies.

In addition to the illustration seen at Figure 8, the sensors that seemed to have the best separation between the reference and added ion samples were confirmed by the examination of raw signal data. With performing the measurement several consecutive times, the final sensors were determined for experimental part II.

3.2.2 Synthetic sample measurements

In the preliminary sensor screening phase of the experimental part I (Section 3.2.1) simple analyte samples were measured that contained only one added ion (barium,

calcium or sulphate). By using the algorithm difference plot, it was possible to rule out sensors that were not providing relevant information about the measured samples.

The next phase of the experimental part I was to continue the assessment with complex samples. Complex samples in this project were a combination of the given ions of barium, calcium and sulphate. All of the sensors found suitable with the simple analyte samples were again analysed with a set of complex samples. After the complex samples were analysed, a set of best sensors for detecting given ions were determined. As a result of this data mining and analysis in experimental part I, the amount of sensor elements was reduced from 24 192 to 885 most suitable. A sensor in this context denotes for the combination of a sensor chemistry and specific excitation-emission wavelength.

4 Experimental part II

In experimental part II, the 885 most suitable sensors were used to develop a predictive model that could be used to analyse time-resolved fluorescence signal responses from produced water samples. During experimental part II, the number of suitable sensors were further reduced into 16 best sensors with the highest explanatory power.

The experimental part II is presented with three sections. The following Section 4.1 addresses the preliminary configuration challenges before constructing the actual Generalized Linear Model (GLM). Section 4.2 handles the background and implementation of the predictive model that was used in this thesis project to determine ion concentrations from four different produced water samples. Section 4.3 presents the actual measurement procedure for performing analytical ion concentration determination from the given produced water samples.

4.1 Prediction model configuration

At the beginning of the experimental part II, the number of possible sensors were reduced into 885. At this phase, it was clear that all of these sensors had a response differential between the reference and analyte sample, although the actual response magnitude had not been yet determined. Therefore, all sensor responses were analysed with correlation coefficients, response plots and signal range evaluation. Both Pearson and Spearman correlation coefficients were used to describe the signal concentration responses. This analysis phase was mainly conducted by hand. Going through the data by hand ensured that the final sensor evaluation was made reliably and the selected sensors had divergent response to different ions. The response or sensitivity was not fully specific towards single ion. This behaviour is discussed later in this chapter and the results are presented at Section 5.1.

4.2 Prediction model preparation

A prediction model in this thesis framework was a mathematical model that used independent variables to explain a continuous variable under examination. A generalized linear model (GLM) was found to be the most suitable method. The GLM was created and performed with RStudio version 0.99.473 (R Core Team, 2015).

As the name implies, GLM is based on the classical linear model wherein the dependent variable behaviour can be predicted as a function of independent variables. However, although the predictive power of linear models are found suitable in many situations, there are some disadvantages. These disadvantages include the assumption of dependent variable continuity, approximate normal distribution and the variance homoscedasticity (Dunteman & Ho 2006). With generalized linear models, these disadvantages are disregarded and the behaviour can be modelled without the restrictions listed above. GLMs have three governing components, which are described by Hox (2010) as:

1. predicted variable error distribution with a mean μ and variance σ^2
    - usually formulated as $y \sim N(\mu, \sigma^2)$
2. a linear additive regression equation that produces a latent predictor η of the outcome variable
    - $\eta = \beta_0 + \beta_1 X_1 + \beta_2 X_2 + \ldots + \beta_n X_n$
3. a link function that combines the expected values to the predicted
    - identity function $\eta = \mu$.

Therefore, the Generalized Linear Model function can be simplified to following equation:

$$Concentration \sim \sum_{i=1}^{n} Sensor\ element_i + \varepsilon \qquad \textit{Equation 2}$$

, where the ion concentration (response variable) is predicted as the sum of sensor element responses (explanatory variables) and an error factor. The error factor contains both systematic and random error elements, which were determined from the measurement dataset.

In Equation 2, the concentrations are predicted individually for each ion. Because sensors were differently responsive to ions, the resulting GLM consisted of sensors that had different explanatory power over each ion. Hence, some redundant information was present in the GLM.

The construction of a prediction model with both synthetic and produced water samples had two separate stages. First, a calibration or "teaching" data set was used to create the GLM and then the created GLM was used to predict concentrations for another data set. With produced water samples, the calibration data and produced water measurement data was separated into two data files. However, this was not needed for the first GLM, because it was only using the synthetic sample information to test the functionality of the GLM. The GLM functionality testing was conducted to identify the response of the GLM predictions to different ion concentration ratios and to analyse the accuracy of the measurement results against the ICP-OES measurements. In this GLM, the raw measurement data was randomly divided with an R-script

into two parts: GLM training data set (70% of the full data set) and the prediction data set (the remaining 30%). Appendix 4 presents the used R code and parameters.

After the functionality of the GLM was tested with synthetic samples, the GLM was used for the produced water samples. Similar to synthetic data GLM, the final prediction model for real samples had two separate input data files, however, the difference was that predicted (produced water measurement) data set had no information about the sample concentrations.

4.3 Produced water sample measurements

The measurements conducted upon the real produced water samples were the main target of this thesis project. Therefore, it was imperative to have a reliable comparative data to verify the functionality of the time-resolved fluorescence assay. The comparative experiments were performed with ICP-OES at the Department of Chemistry in Aalto university. A set of four different produced water samples were provided by Aqsens Oy. These samples were analysed with both ICP-OES and the developed TRF-assay.

Because in the GLM functionality testing phase the measurement range was set to 100–500 ppm, the real produced water samples had to be diluted to the same range. The produced water sample concentrations for calcium were 3140; 2840; 4120; 282 ppm for produced water samples PW1–PW4 respectively (Table 8). This meant that the produced water samples PW1–PW3, were diluted to a series between 100–500 ppm and the produced water sample PW4 was diluted between 100–282 ppm range.

5 Results and discussion

The results of this thesis can be summarized with three topics: data screening process for analysing a large number of possible sensors, the methods to select suitable sensors for the prediction model, and the final method (prediction model) and its performance. The following sections present the results gained during this thesis and discusses the meaning against the topics listed above.

5.1 Sensor selection for prediction model

Figure 9 presents an example of two sensors that are responding differently to the varying ion concentrations. As the signal is changing as a function of concentration, the sensors presented at Figure 9 were suitable for prediction model. All sensors that did not have strong response to the varying concentration were omitted by the examination of response plots and correlation coefficients. As a result of this phase, 16 modulators were selected to the prediction model.

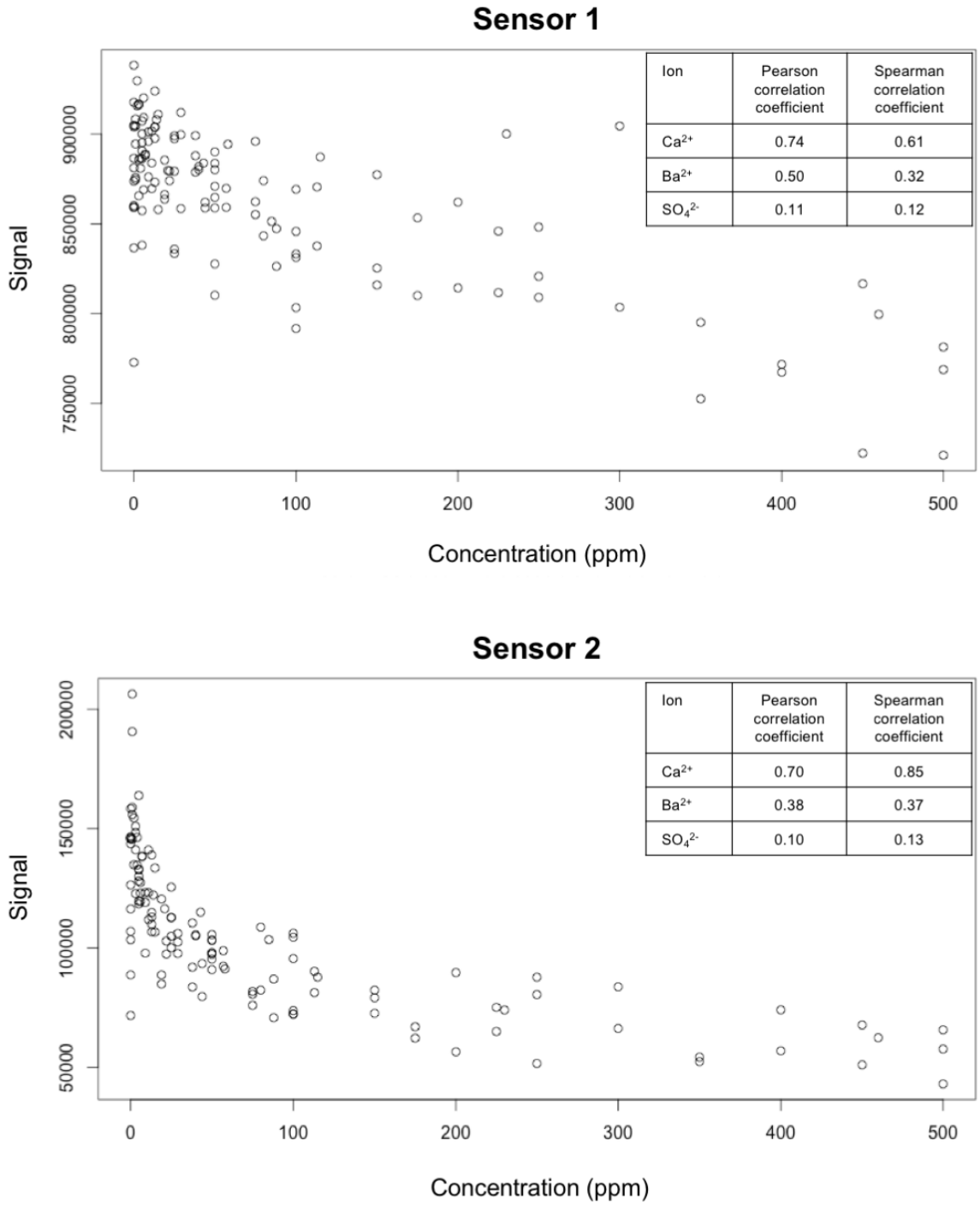

Figure 9 - A sensor signal response against varying ion calcium concentration

After the evaluation phase presented at Figure 9 was complete, the remaining 16 sensors were found to be suitable explanatory variables for the GLM. Table 8 presents the response of final 16 sensors to each, where the normalized slope (sensitivity) of a sensor illustrates the explanatory power for a specific ion. Equation 3a and 3b explain how the slope values presented at Table 8 were calculated.

$$a_{ion} = \frac{\sum(x - \bar{x})(y - \bar{y})}{\sum(x - \bar{x})^2}$$ *Equation 3a*

, where the slope of the regression line (a) is calculated from the signal means (x) and the corresponding concentration means (y).

$$normalized\ ion\ sensitivity_{ion} = \frac{(a_{ion} - \min(a_{all\ ions}))}{(\max a_{all\ ions} - \min(a_{all\ ions}))}$$ *Equation 3b*

, where the slope regression line coefficients (a) are normalized against the slope lines for each ion.

A slope value of zero denotes that the sensor has low separation for different concentrations. The slope values are normalized for each sensor separately, thus it is possible to determine which sensors are responsive to what ion.

Table 8 - Normalized slopes for 16 sensors used in the ion assay

Ion / Sensor no.	1	2	3	4	5	6	7	8	9	10	11	12	13	14	15	16
Ca^{2+}	0	0,6	1	0,3	1	0,1	1	1	1	0,9	0,2	0	1	0,5	0,2	1
Ba^{2+}	0,8	1,0	0	1	0	0	0,3	0	0	1	0	1	0,4	0	1	0
SO_4^{2-}	1,0	0	0	0	0	1	0	0,6	0,8	0	1	0,3	0	1	0	0

Sensor sensitive to ion

From Table 8, it can be seen how the GLM uses the measurement information to construct the prediction model. Each sensor is always sensitive either to one or two ions. Combining this response information produced by different sensors, the prediction model was able to assess the concentration for a given analyte.

5.2 ICP-OES measurements for synthetic and produced water samples

In this thesis, ICP-OES technique was selected for alkaline earth metal content measurements (calcium and barium) from a set of synthetic and produced water samples.

The ICP-OES results provided the comparative information against the measurement method developed in this thesis.

Table 9 presents the results from the ICP-OES measurement for the alkaline earth metal components (calcium and barium). In addition to real produced water samples, a set of synthetic samples were measured to analyse the calibration data accuracy. The calibration data was used to "teach" GLM to predict the different concentrations from a produced water sample.

Table 9 – A set of samples tested with ICP-OES and the corresponding results

Sample ID	Target sample composition (mg/dm^{-3})			ICP-OES results (mg/dm^{-3})		
	Calcium	Barium	Sulphate	Calcium	Barium	Sulphate
Synthetic samples						
Sample 1	500	500	0	553	565	nd
Sample 2	50	50	0	56	56	nd
Sample 3	5	5	0	10	5	nd
Sample 4	500	0	500	662	< 1	nd
Sample 5	50	0	50	55	< 1	nd
Sample 6	300	50	0	340	49	nd
Sample 7	300	0	50	343	< 1	nd
Sample 8	100	400	0	103	452	nd
Sample 9	50	0	300	53	< 1	nd
Sample 10	50	300	0	48	323	nd
Sample 11	350	0	200	378	< 1	nd
Real produced water samples						
Sample 12	unknown			282	< 1	nd
Sample 13	unknown			3140	< 1	nd
Sample 14	unknown			2840	< 1	nd
Sample 15	unknown			4120	< 1	nd

nd = not defined

As a result of the ICP-OES measurements, calcium and barium concentrations were determined. The results presented at Table 9 indicate that barium was not present in the real produced water samples. Therefore, the develop TRF-assay was only used for calcium determination from produced water samples.

5.3 Synthetic sample prediction model results

The final synthetic sample measurement results are presented at Figure 10. The figure lists prediction model results for calcium, barium and sulphate separately. In addition to the comparative data between the predictions and the actual concentrations, a recovery trendlines are presented at the graphs. The recovery trendlines describe the 20% deviation from the actual concentrations.

As for the results, it can be seen from Figure 10 that all three synthetic sample predictions had good accuracy. Therefore, it seems that the GLM was able to separate all three ions from a synthetic sample in the given range of 100–500 ppm. Although some prediction variation was present, a positive aspect was that the results were gained by using the same assay set-up for all ions. The same assay set-up in this context meant that the selected 16 sensors and GLM remained unchanged in all of the ion determination measurements.

Therefore, the experiments with the synthetic samples provided a suitable model to predict the concentrations from a known sample matrix. With this test, the GLM performance was found to provide reasonable accurate results and thus, it should be able to predict the concentrations from a set of real samples. The results from a produced water measurements are presented at Section 5.4.

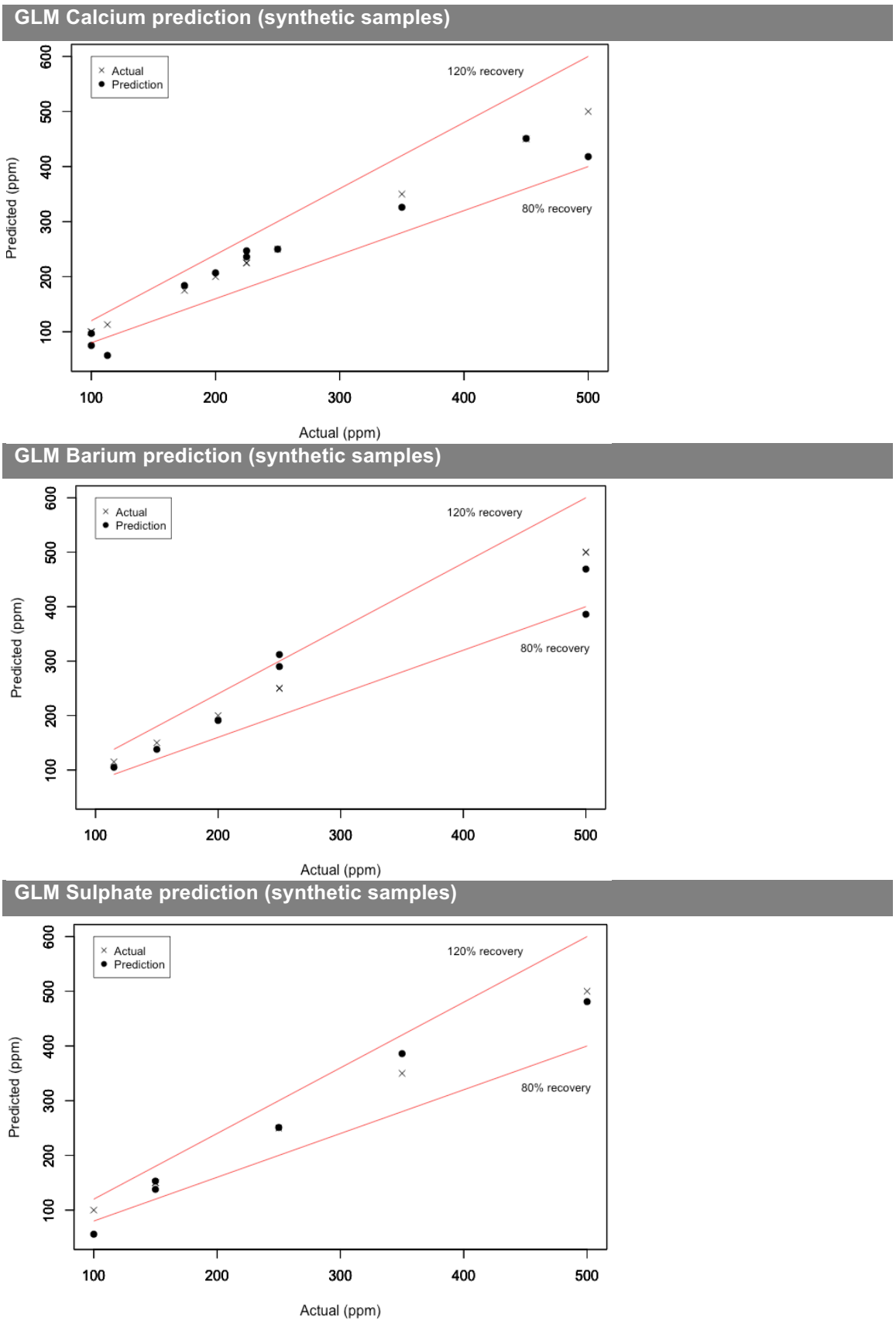

Figure 10 - GLM results from synthetic sample measurements

As described earlier, the GLM used in synthetic sample measurements consisted of complex synthetic samples that had a varying concentrations of all three ions (calcium, barium and sulphate). The aim was to asses the level of distortion when a high analyte to second ion ratio was present. Significant variation was not found from these prediction models. Table 10 presents the predicted data points (30% of the full data set) and the related disruptive ion concentrations for these samples.

Table 10 - GLM results and the actual values for each ion present in the sample matrix

Synthetic sample GLM results, Calcium			
Predicted Ca^{2+} [mg/dm^{-3}]	**Actual Ca^{2+}** [mg/dm^{-3}]	**Actual Ba^{2+}** [mg/dm^{-3}]	**Actual SO_4^{2-}** [mg/dm^{-3}]
418	500	0	0
451	450	150	0
326	350	460	0
250	250	0	250
236	225	0	75
247	225	75	0
207	200	0	100
184	175	230	0
57	113	0	38
75	100	0	100
97	100	400	0
Synthetic sample GLM results, Barium			
Predicted Ba^{2+} [mg/dm^{-3}]	**Actual Ba^{2+}** [mg/dm^{-3}]	**Actual Ca^{2+}** [mg/dm^{-3}]	**Actual SO_4^{2-}** [mg/dm^{-3}]
469	500	0	0
386	500	100	0
290	250	0	0
312	250	250	0
191	200	400	0
138	150	450	0
105	115	88	0
Synthetic sample GLM results, Sulphate			
Predicted SO_4^{2-} [mg/dm^{-3}]	**Actual SO_4^{2-}** [mg/dm^{-3}]	**Actual Ca^{2+}** [mg/dm^{-3}]	**Actual Ba^{2+}** [mg/dm^{-3}]
481	500	0	0
386	350	460	0
251	250	50	0
138	150	85	0
153	150	450	0
56	100	0	0

As can be seen from the results in Table 10, the added ions were not significantly affecting the predicted values. However, especially for barium and sulphate, the number of observations was low and therefore, larger experiments should be conducted to confirm the findings. Despite this, the main conclusion about the synthetic sample prediction test was that the GLM model is indeed sensitive to analytes of interest and the developed model should be able to predict ion concentrations from real produced water samples.

5.4 Produced water prediction model results

For produced water sample measurements, a calibration data set was extracted from Section 5.2 measurements. This synthetic data provided a training data set for the real produced water samples discussed in this section.

For this measurement, four different produced water samples were collected from Aqsens Oy sample storage. For all of these samples, an ICP-OES measurement was conducted to determine the calcium and barium concentrations. Table 9, presents the ICP-OES results for all samples; synthetic and produced water. According to the results obtained with ICP-OES, it was decided that calcium determination would provide most information about the prediction model performance. The performance was evaluated from the results presented at Figure 11. The figure presents the prediction model results for all of the measured produced waters. For PW1, PW2 and PW3, the prediction results met the concentration determined with ICP-OES fairly well, however with PW4, the predicted concentrations were much higher than the actual concentration determined with the ICP-OES.

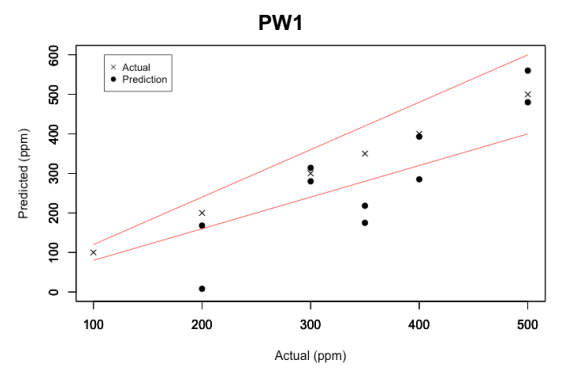

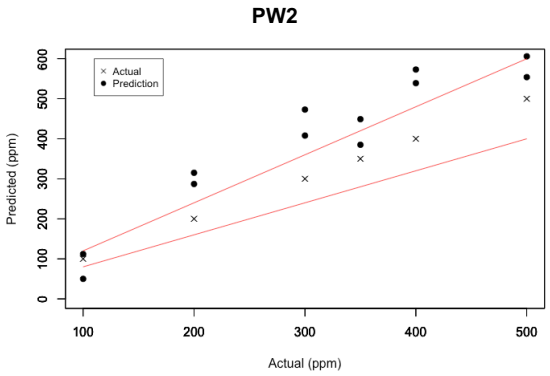

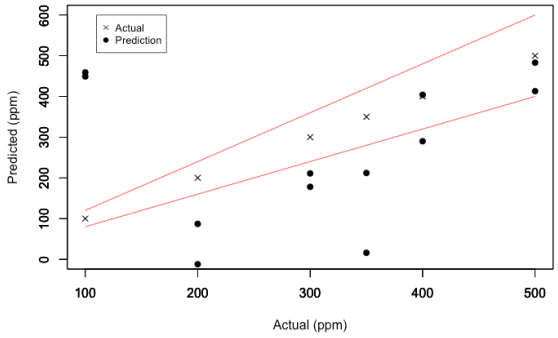

PW4

Actual concentration (ppm)	Predicted concentration (ppm)
282	1561
282	1657
250	1488
250	1481
225	1474
225	1579
150	1097
150	1073
100	645
100	722

Figure 11 - GLM prediction results for produced water samples

As can be seen from Figure 11, with produced water samples PW1, PW2 and PW3, the performance of the GLM seemed to be decent only with concentrations above 300 ppm. Identical behaviour was examined when GLM was using the range between 0–500 ppm. The result indicated that the GLM had difficulties to predict concentrations below 100 ppm. This problem is mainly due to the sensor cross-reactivity, which produces high variability to the measured signals in the low concentration levels. This was the same even with synthetic samples, thus the produced water predictive model measurement range was set to 100–500 ppm.

Table 11 - GLM prediction and ICP-OES result comparison table for PW1

Actual Ca^{2+} [mg/dm^{-3}]	Predicted Ca^{2+} [mg/dm^{-3}]	Dilution factor	GLM Ca^{2+} prediction $[Prediction * Dil.factor]$ [mg/dm^{-3}]	ICP-OES Ca^{2+} result [mg/dm^{-3}]
500	560	6,28	3517	3140
500	480	6,28	3014	
400	393	7,85	3085	
400	285	7,85	2237	
350	218	8,97	1955	
350	175	8,97	1570	
300	280	10,47	2932	
300	314	10,47	3288	
200	168	15,70	2638	
200	8	15,70	126	
100	-215	31,40	-6751	
100	-258	31,40	-8101	

Table 11 presents the dilution series for the PW1 and the corresponding predicted values. As can be seen from Table 11, when the diluted values are transformed back to the original concentrations by using the dilution factors, the measured results for higher concentrations of 400–500 ppm are predicting the concentration of calcium with reasonable accuracy. As for the lower concentrations this is not the case and the prediction model seems to misinterpret concentrations under 400 ppm range. This conclusion might also explain the PW4 results. The PW4s predicted concentrations are much higher than the actual concentrations. The highest sample concentration for PW4 was 282 ppm; thus was is less than the suitable performance limit of 400 ppm.

5.5 Method performance

The method performance had two aspects: sensor validation performance and the predictive model performance. The sensor validation was the starting point for this thesis and it defined the needed components and parameters to detect different ions. Therefore, the sensor validation and selection was determining the performance for the prediction model. Without proper sensors, the functionality of the predictive model would have been decreased.

According to the results of this thesis, by using the developed sensor validation method, suitable sensors were found. This conclusion is supported by the results in Sections 5.3 and 5.4, where both synthetic and produced water sample results are uniform with the ICP-OES results.

However, although suitable sensors were found for the prediction model, it is possible that during the sensor evaluation process some of the sensors with high explanatory power were omitted accidently. However, albeit few suitable sensors would have been omitted, the model performance was not significantly reduced, because several sensors are needed to perform the measurement. Therefore, omitting a single response entity will not affect the prediction model performance in a significant way.

As for the results from predictive model, it can be said that the model was working reasonably well with three produced water samples (PW1; PW2; PW3). However, PW4 shows similar behaviour, but the predicted concentrations are much higher than actual concentrations. This behaviour might be due to the low original concentration of PW4 (282 ppm), which was lower than the method performance. In addition to the low calcium concentration of PW4, the dilution may have affected the results. All of the other samples were diluted, whereas PW4 had no dilution. Therefore, a likely explanation is the sample matrix impurities inflicted interference to the measurement signal.

Nevertheless, the predictive model results suggest that it is possible to answer the experimental question set at the beginning of this thesis. The experimental problem for this thesis was the detection of scale causing components form a produced water sample matrix. Although, as described by the literature review of this thesis, the produced water composition is a highly variable sample matrix, the performance of the predictive model can be considered as a success. However, much development could be conducted to enhance the performance and repeatability of the ion concentration determination method. In addition to repeatability, the prediction model performance should be also studied further on to concentrations below 100 ppm.

To achieve better performance a throughout knowledge about the interactions related to the sensors should be studied. This work would enhance the predictive power of the GLM and therefore improve the reliable measurement range and sensitivity.

5.6 Scale potential assessment

In addition to the analysis of the gained results, it was also important to address the question of possible end application. An end application is already described in the introduction part of this thesis. The application should provide a solution to detect and analyse scale causing components from a produced water samples, in order to provide information from an oil production process stream. However, the knowledge about ion concentrations alone is not enough. As the method is presenting the results in ion concentrations (ppm), it is more useful to combine the information about the component concentrations into scale potential assessment. Therefore, graphs at Appendix 2 are presenting the relationship of the given scale causing components and the severity of scaling as an accumulation of scale per cubic meter of water. As it is clear, one ion does not pose a scale problem. Problems arise when ions form ionic bonds with low solubility components. In Appendix 2, especially harmful scale is the Barite scale that forms precipitates in rather low concentrations. Calcium sulphate precipitates in higher components concentrations, however, with combined to other precipitates it may cause high risk of scale accumulation.

As stated, the information about the specific concentrations in the produced water stream is valuable information, although the topic has to be put into a wider perspective. This means that, although it is possible to develop a fast and easy-to-use measurement application, the method is a complementary measurement for providing information about the oil production process. Therefore, the information can be used as a supporting material, for example, scale inhibitor program design or to assess the scale potential in general level. The method developed during this thesis is therefore more of a surveillance method and the actual control has to be decided as an ensemble of measurement and follow-up procedures.

6 Conclusions

This thesis explains in three phases how time-resolved fluorescence method can be used to identify several different ion species from a liquid sample. These three phases included methods to evaluate large number of different sensor chemistries, a protocol to use small number of sensor chemistries for creating differential responses from samples and a system to interpret these measured responses. The results of this thesis indicated that if carefully selected sensors were mixed with a chelate-sample solution, it was possible to create a predictive model that was able to convert the signal responses into an estimation of sample ion concentration. This thesis presented the methodology to perform the sensor analysis through data handling methods and how to use the selected sensors to predict analyte concentrations from a produced water sample.

As the ion concentration determination was possible with the method developed, this information could be used, for example, supporting material for scale inhibitor program or scale potential assessment in a general level. The results suggest that the developed methods could be used as a complementary measurement to evaluate the risks related to different aqueous components within an oil extraction process.

Although it was shown that with the method developed it is possible determine ion concentrations from a sample matrix, much improvement can be achieved through further studies. One aspect could be the sensitivity of the measurement system. By studying the interactions between a sensor and sample, as well as optimising the measurement environment and parameters, it should be possible to enhance the sensitivity of the measurement system. The increased sensitivity would provide more accurate measurement results and may extend the measurement range to concentrations below 100 ppm.

References

Albani, J.R. 2007, "*Principles and applications of fluorescence spectroscopy".* Blackwell Science, Oxford; Ames, Iowa.

Alzahrani, S. & Mohammad, A.W. 2014, "Challenges and trends in membrane technology implementation for produced water treatment: A review", *Journal of Water Process Engineering,* vol. 4, no. 0, pp. 107-133.

Anzenbacher, P., Lubal, P., Bucek, P., Palacios, M.A. & Kozelkova, M.E. 2010, *"A practical approach to optical cross-reactive sensor arrays".* Chemical Society reviews, Vol.39(10), pp.3954-79.

Bezerra, M.A., Mitihiro do Nascimento Maêda, S., Oliveira, E.P., de Fátima Batista de Carvalho,Maria & Santelli, R.E. 2007, *"Internal standardization for the determination of cadmium, cobalt, chromium and manganese in saline produced water from petroleum industry by inductively coupled plasma optical emission spectrometry after cloud point extraction"*. Spectrochimica Acta Part B: Atomic Spectroscopy, vol. 62, no. 9, pp. 985-991.

Boitsov, S., Meier, S., Klungsøyr, J. & Svardal, A. 2004, *"Gas chromatography–mass spectrometry analysis of alkylphenols in produced water from offshore oil installations as pentafluorobenzoate derivatives"*. Journal of Chromatography A, vol. 1059, no. 1–2, pp. 131-141.

Dórea, H.S., Bispo, J.R.L., Aragão, K.A.S., Cunha, B.B., Navickiene, S., Alves, J.P.H., Romão, L.P.C. & Garcia, C.A.B. 2007, *"Analysis of BTEX, PAHs and metals in the oilfield produced water in the State of Sergipe, Brazil"*. Microchemical Journal, vol. 85, no. 2, pp. 234-238.

Dunteman, G.H. & Ho, M.R. 2006, "*An introduction to generalized linear models".* SAGE, London.

Fakhru'l-Razi, A., Pendashteh, A., Abdullah, L.C., Biak, D.R.A., Madaeni, S.S. & Abidin, Z.Z. 2009, *"Review of technologies for oil and gas produced water treatment"*. Journal of Hazardous Materials, Vol.170(2), pp.530-551.

Dickson, E.F.G., Pollak, A. & Diamandis, E.P. 1995, *"Time-resolved detection of lanthanide luminescence for ultrasensitive bioanalytical assays".* Journal of Photochemistry & Photobiology, B: Biology, Vol.27(1), pp.3-19.

Hagan, A.K. & Zuchner, T. 2011, "Lanthanide-based time-resolved luminescence immunoassays". Anal Bioanal Chem, vol. 400, no. 9, pp. 2847-2864.

Hänninen, P.E., Siivonen, J.J., Väisänen, P.I., Tiittanen, S.A., Lehmusto, M.M., Teimonen, T., Törnkvist, N., Sandell, M.A., Knaapila, A.J., Mundill, P. & Härmä, H.J. 2013, *"Fuzzy liquid analysis by an array of nonspecifically interacting reagents: the taste of fluorescence"*. Journal of the American Chemical Society, Vol.135(20), pp.7422-5.

Hox, J.J. 2010, *Multilevel analysis : techniques and applications,* 2nd ed. edn, Routledge, New York.

Igunnu, E.T. & Chen, G.Z. 2014, *"Produced water treatment technologies"*. International Journal of Low-Carbon Technologies, vol. 9, no. 3, pp. 157-177.

Kelland, M.A. 2014, "*Production Chemicals for the Oil and Gas Industry".* Second Edition edn, CRC Press.

Lee, K. & Neff, J. 2011, "*Produced Water: Environmental Risks and Advances in Mitigation Technologies".* Springer, New York.

Mukkala, V., Helenius, M., Hemmilä, I., Kankare, J. & Takalo, H. 1993, *"Development of Luminescent Europium(III) and Terbium(III) chelates of 2,2?:6?,2?- terpyridine derivatives for protein labelling"*. Helvetica chimica acta, vol. 76, no. 3, pp. 1361-1378.

PerkinElmer Inc. 2015, "*Time-resolved fluorometry and DELFIA"*. Available: http://www.perkinelmer.com/pages/020/staticpages/time-resolvedfluorometryanddelfia.xhtml [Accessed: 12.10.2015].

RStudio Team. 2015, "*RStudio: Integrated Development Environment for R"*. Inc., Boston, MA. Available: http://www.rstudio.com/ [Accessed: 30.10.2015].

Ray, J.P. & Engelhart, F.R. (eds) 1992, "*Produced Water"*. 1st edn, Springer US.

Røe Utvik, T.I. 1999, *"Chemical characterisation of produced water from four offshore oil production platforms in the North Sea"*, Chemosphere, vol. 39, no. 15, pp. 2593-2606.

Siivonen, J.J., Väisänen, P.I., Tiittanen, S.A., Lehmusto, M.M., Lehtonen, P., Patrikainen, E., Teimonen, T., Törnkvist, N., Mundill, P., Hänninen, P. & Härmä, H. 2014, *"Novel non-specific liquid fingerprint technology for wine analysis: a feasibility study".* Australian Journal of Grape and Wine Research, Vol.20(2), pp.172-177.

Skoog, D.A. 2007, "*Principles of instrumental analysis".* 6th ed. edn, Brooks/Cole, Belmont, CA.

Veil, J.A., Puder, M.G., Elcock, D. & Redweik, R.J. 2004, "*A White Paper Describing Produced Water from Production of Crude Oil, Natural Gas, and Coal Bed Methane"*. Argonne National Laboratory.

Yuan, J. & Wang, G. 2005, *"Lanthanide Complex-Based Fluorescence Label for Time-Resolved Fluorescence Bioassay".* Journal of Fluorescence, Vol.15(4), pp.559-568.

Zumdahl, S.S. & Zumdahl, S.A. 2000, "*Chemistry".* 5. ed. edn, Houghton Mifflin, Boston (MA).

Appendices

Appendix 1 Data handling algorithm flow chart (1 page)

Appendix 2 Calculated theoretical precipitation equilibrium and estimated precipitation accumulation for Barite and calcium sulphate (1 page)

Appendix 3 Sensor composition and identification table (1 page)

Appendix 4 R code and parameters for Generalized Linear Model (2 pages)

Appendix 5 Sensor components and identification table (1 page)

Appendix 1. Data handling algorithm flow chart

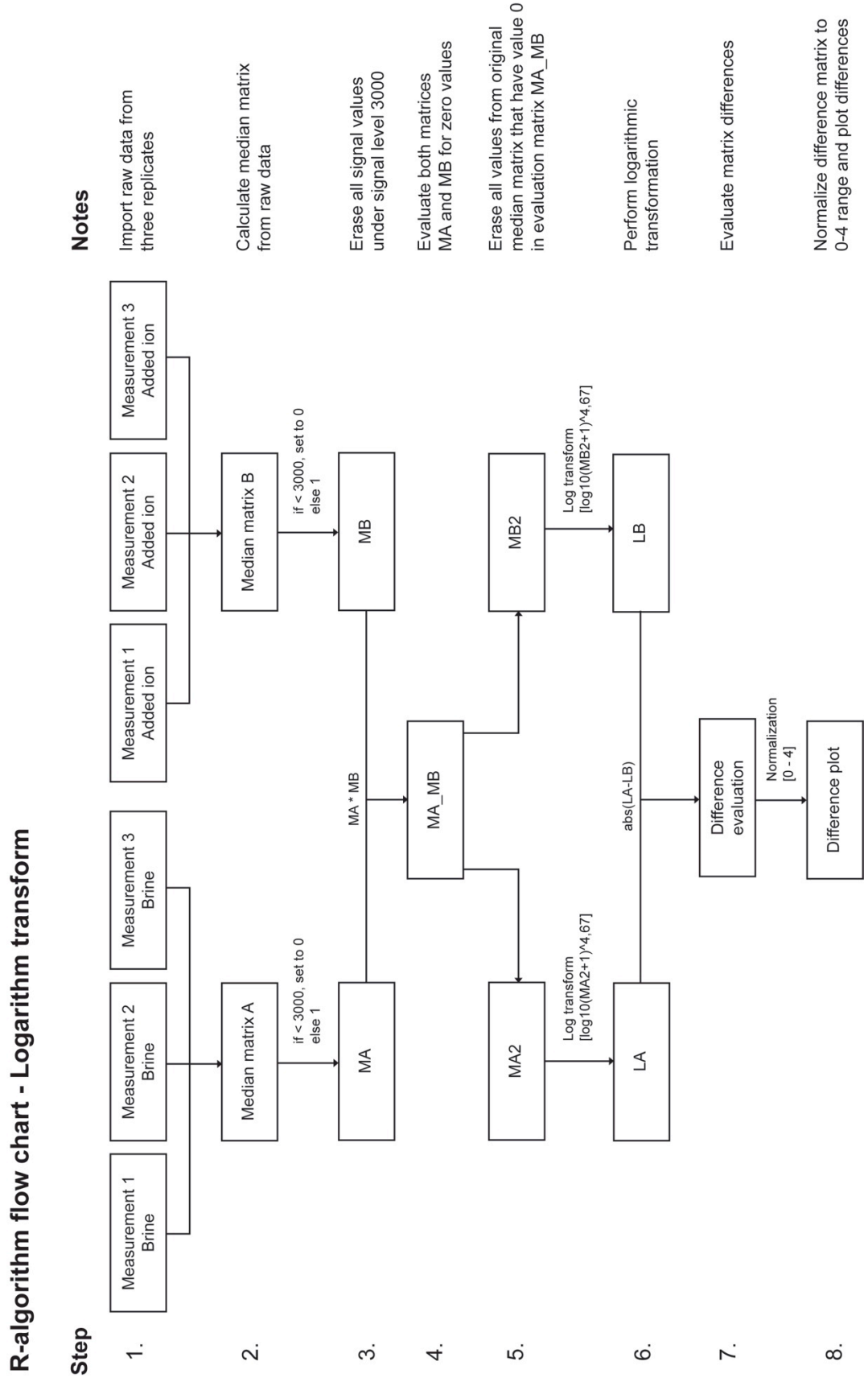

Appendix 2. Calculated theoretical precipitation equilibrium and estimated precipitation accumulation for Barite and Calcium sulphate

Precipitation limit and scale accumulation for Calcium sulfate ($CaSO_4$)

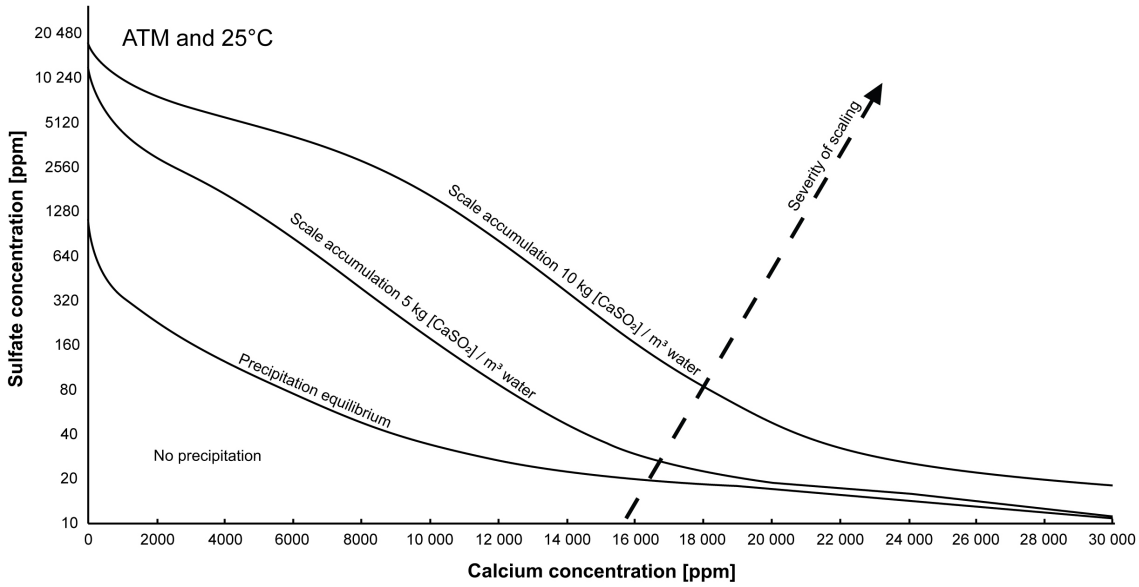

Precipitation limit and scale accumulation for Barite ($BaSO_4$)

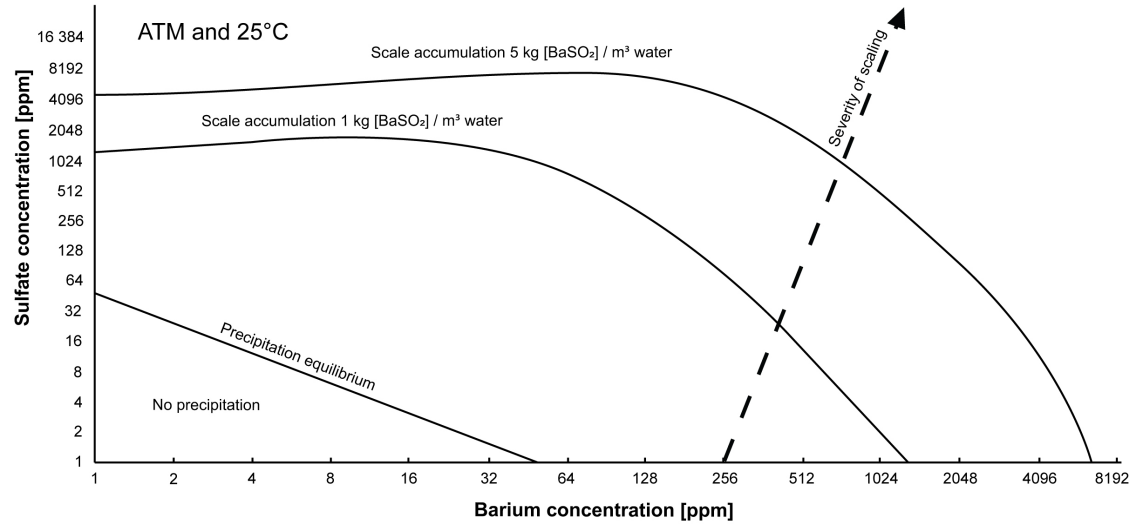

(Zumdahl, Zumdahl 2000)

Appendix 3. Sensor composition and identification table

	Sensor				
Sensor ID	**Ionochromic dye**		**Modulator**	**Excitation wavelength (nm)**	**Emission wavelength (nm)**
B1	A13	+	A15	250	620
B2	A13	+	A15	270	600
B3	A13	+	A15	300	615
B4	A13	+	A15	310	590
B5	A13	+	A15	310	615
B6	A13	+	A15	310	620
B7	A4	+	A16	300	615
B8	A4	+	A16	310	615
B9	A4	+	A16	340	615
B10	A6	+	A15	320	600
B11	A6	+	A15	330	615
B12	A2		-	310	615
B13	A2		-	330	595
B14	A2		-	330	625
B15	A2		-	340	615
B16	A2		-	340	620

Appendix 4. R code and parameters for Generalized Linear Model

```
######################## DATA IMPORT ############################
train_ca <- read.csv(("train_data.csv"), header=T)
predict_ca <- read.csv(("predict_data_PW1.csv"), header=T)


######################## BUILD GLM ##############################
conc.glm <- glm(formula=Ca~., data=train_ca, family="gaussian")


######################## PREDICTION START #######################

######### Random data partition for synthetic sample measurements
#sample_ids <- nrow(predict_ca)
#sub <- sample(sample_ids, floor(sample_ids) * 0.70)
#teach_ids <- predict_ca[sub,]
#test_ids <- predict_ca[-sub,]

######### Prediction results
# Results table column 1
results <- as.data.frame(round(predict.glm(conc.glm, predict_ca),digits = 0))
# Results table column 2, actual concentrations
results[,2] <- predict_ca$Ca
# Results table column 3, Recovery (variation from actual concentration)
results[,3] <- round(((results[,1]/results[,2])),digits=2)

######### Observation concentrations
Observations <- predict_ca[,1]

######### 20 percent deviation plot
pos <- cbind(Observations,(0.2*results[,2]+results[,2]))
neg <- cbind(Observations,(results[,2]-(0.2*results[,2])))

######### Plot
plot(Observations, results[,1], pch=19, type="p", ylab="Predicted (ppm)",
xlab="Actual (ppm)", ylim = c(0,600), xlim = c(100,500))
par(new=TRUE)
plot(Observations, predict_ca[,1], main="PW1",pch=4,type="p", ylab="",
xlab="", lwd="1", ylim = c(0,600), xlim = c(100,500))
par(new=TRUE)
plot(Observations, pos[,2],col="red", type="l", ylab="", xlab="", lwd="1",
ylim = c(0,600), xlim = c(100,500))
par(new=TRUE)
plot(Observations, neg[,2],col="red", type="l", ylab="", xlab="", lwd="1",
ylim = c(0,600), xlim = c(100,500))

legend(110, 600, pch=c(4,19), col=c("black", "black"),
c("Actual","Prediction"), bty="o", cex=.8)

######################## PREDICTION END #########################
```

```
Call:
glm(formula = Ca ~ ., family = "gaussian", data = train_ca)

Deviance Residuals:
     Min        1Q    Median        3Q       Max
-135.312   -30.376     1.495    38.420   119.267

Coefficients:
            Estimate    Std. Error  t value     Pr(>|t|)
(Intercept) 2.673e+03   2.053e+02   13.024      < 2e-16 ***
B1          -1.851e-03  1.384e-03   -1.338      0.188068
B2          2.001e-03   2.633e-03   0.760       0.451355
B3          3.669e-04   6.683e-04   0.549       0.585809
B7          -6.472e-04  3.569e-04   -1.813      0.076744 .
B4          1.619e-03   2.549e-03   0.635       0.528634
B5          -1.035e-03  7.049e-04   -1.468      0.149343
B8          -1.328e-04  3.719e-04   -0.357      0.722766
B12         -3.246e-04  3.922e-04   -0.828      0.412492
B6          1.665e-04   4.041e-04   0.412       0.682285
B10         6.242e-03   2.663e-03   2.344       0.023767 *
B13         -5.384e-05  1.208e-03   -0.045      0.964640
B11         -3.939e-03  1.437e-03   -2.741      0.008881 **
B14         -9.912e-04  1.463e-03   -0.677      0.501786
B9          4.253e-04   6.988e-04   0.609       0.545970
B15         -1.767e-03  4.841e-04   -3.649      0.000707 ***
B16         -2.018e-03  9.050e-04   -2.230      0.031034 *
---
Signif. codes:  0 '***' 0.001 '**' 0.01 '*' 0.05 '.' 0.1 ' ' 1

(Dispersion parameter for gaussian family taken to be 3619.518)

    Null deviance: 1080994  on 59  degrees of freedom
Residual deviance:  155639  on 43  degrees of freedom
AIC: 677.93

Number of Fisher Scoring iterations: 2
```